The kinetic plot method applied to gradient chromatography: theoretical framework and experimental validation

K. Broeckhoven[1], D. Cabooter[1], F. Lynen[2], P. Sandra[2] and G. Desmet[1,*]

(1) *Vrije Universiteit Brussel, Department of Chemical Engineering, Pleinlaan 2, 1050 Brussels, Belgium*

(2) *Dept. of Organic Chemistry, Universiteit Gent, Krijgslaan 281 S4-Bis, 9000 Gent, Belgium*

* Corresponding author. Pleinlaan 2, 1050 Brussels, Belgium.

Phone: (+)32.(0)2.629.32.51. Fax: (+)32.(0)2.629.32.48. E-mail: gedesmet@vub.ac.be

Keywords: kinetic performance, gradient elution, band broadening, peak compression, numerical simulation

Abstract

The kinetic plot method, originally developed for isocratic separations, was extended to the practically much more relevant case of gradient elution separations. A set of explicit as well as implicit data transformation expressions has been established. These expressions can readily be implemented in any calculation spread-sheet program, and allow to directly turn any experimental data set representing the relation between the separation efficiency and the flow rate measured on a single column into the kinetic performance limit curve of the tested separation medium. Since the kinetic performance limit curve is based on an extrapolation to columns with a different length, it should be realized that the curve is only valid under the assumption that the gradient time and the delay time (if any) are adapted such that the analytes are subjected to the same relative mobile phase history when the column length is changed.

Both experimental and numerical data are presented to corroborate the fact that the kinetic performance limit curves that are obtained using the proposed expressions are indeed independent of the column length the experimental data were collected in. Deviations might arise if excessive viscous heating occurs in columns with a pronounced non-adiabatic thermal behaviour.

1. Introduction

In the pursuit of ever faster or more efficient LC separations, HPLC systems with smaller particles, higher pressures and higher temperatures are currently being developed and commercialized [1-7]. And with the advent of monolithic columns and porous shell particles, also different support formats are being considered [8-10]. To guide this research and the decision analysts have to make when considering the purchase of new systems, a uniform comparison method is needed.

The classical Van Deemter plot does not allow to directly show which approach yields the highest separation resolution in a given time, or which approach yields a given resolution in the shortest possible time (for the general performance of a chromatographic system is also determined by its pressure-drop characteristics). A plot of efficiency or resolution versus the time calculated for the largest available pressure on the other hand directly shows which system would perform best in a given range of required efficiency, resolution or analysis time. Referring to this type of plot with the general name of "kinetic plots", it should be reminded that the use of plots of separation quality versus time already dates back from the classical work of Giddings in 1965 [11]. Knox [12] and Guiochon [13] used the kinetic plot

approach to compare the performance of packed bed columns with open-tubular columns in the seventies and early eighties. In 1997, Hans Poppe proposed to plot t_0/N versus N instead of t_0 versus N to obtain a clearer view on the C-term contribution [14].

Common to the approach adopted by these and other authors [10,15] is that they used a computer optimization or numerical search to find the kinetic optimum. The novelty of the approach presented by our group in 2005 [16] therefore was not a retransformation of the axes (t versus N or t/N^2 versus N instead of t/N versus N), but the presentation of two simple mathematical expressions that allow to turn any experimental data set of H versus u-data (or N versus F-data) directly into a kinetic plot, without the need for a numerical optimization algorithm. The availability of these two simple data transformation expressions (cf. Eqs.(6-7) in Desmet et al. [16]), providing a new and more straightforward way to produce kinetic plots, opened the way to a broad use of kinetic plot comparisons [17,18].

The theory underlying this so-called kinetic plot method (KPM) was however limited to isocratic separations, whereas the majority of the separations is run under gradient elution conditions. Kinetic plots under gradient conditions have recently been presented by Wang et al. and Zhang et al. [10,15], but these plots were still obtained using a computerized constrained optimization algorithm (implemented via a Solver add-in of MS Excel). Mathematical expressions that can directly transform any experimental set of gradient efficiency or peak capacity versus flow rate data directly into a kinetic plot curve are still lacking. The present study therefore aims at providing a theoretical framework to extend the KPM to gradient elution conditions. What results is a broader framework, covering both the isocratic and gradient case, and yielding a set of explicit and implicit data transformation expressions.

2. Separation efficiency measures

Regardless of whether the elution is isocratic or gradient, the efficiency of a chromatographic system can be characterized by a column plate height H or plate count N, which are fundamentally defined [11] with respect to the spatial variance of the bands in the column:

$$H = \frac{\sigma_x^{\,2}}{L} = \frac{L}{N} \qquad (1)$$

Band widths are however usually measured in time and not in space. In that case, the information about H needs to be retrieved from the temporal variance σ_t^2 of the peak observed at the detector. The value of this variance is usually directly calculated by the instrument software, and is linked to H and N via:

$$\sigma_t = \frac{t_0}{\sqrt{N}} \cdot (1 + k_{elut}) = \sqrt{N} \cdot H \cdot \frac{(1 + k_{elut})}{u_0} = \sqrt{L \cdot H} \cdot \frac{(1 + k_{elut})}{u_0} \qquad (2)$$

A key parameter in Eq. (2) is the retention factor (k_{elut}) experienced by the analytes at the moment of elution. Under isocratic conditions, this retention factor is equal to the observed or effective retention factor k (defined as $k=(t_R-t_0)/t_0$) [19-21], so that Eq. (2) can be straightforwardly used to calculate H and N. Under gradient conditions, however, k_{elut} is always smaller than the effective k and can also not be directly measured. In that case, one either needs to determine k_{elut} using the Linear Solvent Strength-model (LSS-model, see Eq. (28)) or any of the more complex mathematical non-LSS models such as those described in [22]. Alternatively, one can first determine the mobile phase composition at which the component elutes and then perform an isocratic elution experiment at this composition to measure k_{elut}. Both approaches anyhow require additional experiments and constitute a potential source of additional measurement errors.

Given this and other complexities, plate heights are seldom used in gradient elution (see the Supporting Material, *SM*, Part 1.1 for a broader discussion of the problems related to the use of the plate height concept under gradient elution elution). Instead, it is often preferred to directly use the observed σ_t or the resulting peak capacity, n_p, as both measures are true "what you see is what you get"-variables.

The peak capacity of a column is most generally expressed in an integral form [23,24]:

$$n_p = 1 + \int_{t_0}^{t_R} \frac{1}{4 \cdot \sigma_t} dt \qquad (3)$$

Eq. (3) can however only be used if the variation of σ_t with the time is exactly known. If this is not the case, the integral can be split up in parts, assuming that the peak width of each eluting band is representative for the range of elution between its own moment of elution and that of the preceding peak [25]:

$$n_p = 1 + \sum_{i=1}^{n} \frac{t_{R,i+1} - t_{R,i}}{4 \cdot \sigma_{t,i+1}} \qquad (4)$$

An even more simplified peak capacity definition is based on the average band width ($w_{p,av}=4 \cdot \sigma_{t,av}$) [23]:

$$\sigma_{t,av} = \frac{1}{n} \cdot \sum_{i=1}^{n} \sigma_{t,i} \qquad (5)$$

$$n_p = 1 + \frac{t_{R,n} - t_1}{4 \cdot \sigma_{t,av}} \qquad (6)$$

Both Eq. (4) and (6) relate to a sample-based peak capacity. Sometimes (as in the present study), the t_0-marker is included as component number i=1, in which case the elution window in Eqs. (4) and (6) extends between t_0 and $t_{R,n}$ (wherein n is the number of sample components +1). In other cases, the peak capacity is calculated based on the gradient time t_G. Yet other peak capacity definitions exist in

literature [15,24,26-28]. All existing n_p-definitions however display the same square-root length-dependency (as shown in the SM, section 2.3), expressed by Eq. (18) further on, so that, for what concerns the application of the KPM, they all behave the same.

In the present work, the definition used in Eq. (4) (with i=1 representing the t_0 marker) has been used throughout all presented figures and data sets. For the sake of clarity, it should also be remarked that the effective retention factor k used in the present study is purely based on the observed peak retention times ($k=(t_R-t_0)/t_0$), for isocratic as well as for gradient elution (the effective k is in the literature on gradient separations k sometimes also denoted as k_g [23]). It should therefore also be noted that k no longer equals the product of the equilibrium constant and the phase ratio in the column in the gradient case.

3. General kinetic plot theory valid for both isocratic and gradient elution

3.1 General concept

The kinetic performance of a chromatographic system can be defined as the efficiency N or peak capacity n_p it can generate in a certain time. This also depends on the permeability of the system, so that the kinetic performance is determined by the three following basic expressions [11,12]:

$$t_0 = \frac{L}{u_0} \tag{7}$$

$$N = \frac{L}{H} \tag{8}$$

$$\Delta P = \frac{u_0 \cdot \eta \cdot L}{K_v} \tag{9}$$

If desired, the efficiency N can be replaced by the peak capacity n_p. In this case, the relation between n_p and σ_t (see e.g., Eq. (4)) and that between σ_t and L (see Eq. (2)) need to be combined into an expression describing n_p as a function of L, and this expression should then replace Eq. (8). This is of course more complicated but nevertheless still leads to a mathematical expression that is straight-forwardly applicable. It might also be preferred to replace the t_0-time by the total time t_R (via $t_R=t_0\cdot(1+k)$) or to replace N by the effective plate number N_{eff} (via $N_{eff}=N\cdot k^2/(1+k)^2$ [16,29]), but these modifications also do not change anything fundamental to the optimization procedure below.

Defining now the kinetic performance limit (KPL) of a given chromatographic support as the set of optimal column lengths and flow rates wherein the complete set of possible N- or n_p- values is achieved

in the shortest possible time, or, equivalently, wherein a maximal N or n_p is achieved over the complete range of possible analysis times, it can be shown (see *SM*, Part 2.1) that both conditions are simultaneously met if the column pressure-drop is equal to the maximally possible or allowable pressure ΔP_{max}:

$$\text{kinetic performance limit is achieved} \Leftrightarrow \Delta P = \Delta P_{max} \quad (10)$$

Putting $\Delta P = \Delta P_{max}$ in Eq. (9) and solving the set of equations given by Eqs. (7-9) hence suffices to calculate the KPL of a given chromatographic support (note that this KPL is only valid for the considered mobile phase and sample, see Section 3.4). Solving Eqs. (7-9) can be done in a purely algebraic manner and leads to the set of explicit kinetic plot expressions shown in the 3rd column of Table 1 (derivation: see Part 2.2 of the *SM*). These expressions transform the efficiency (or n_p or R_s) measured in a column with length L and given flow rate F (and corresponding pressure-drop ΔP) into the efficiency (or n_p or R_s) one would obtain when applying the same velocity or flow rate in a column with a length selected such that $\Delta P = \Delta P_{max}$.

Whereas a Van Deemter curve only contains part of the kinetic information (it lacks the pressure-drop information), the so-called kinetic plot or kinetic performance limit (KPL)-curve directly represents the complete series of optimal kinetic performances (one data point for each possible flow rate) one can expect from a given support under the employed mobile phase conditions. The KPL-curve is therefore ideally suited as a universal performance measure, for example allowing to directly compare monolithic columns with fully and superficially porous particles, in a direct "what you see is what you get" plot.

3.2 Assumptions underlying the validity of the kinetic performance limit curve

Any established KPL-curve in fact corresponds to a prediction of the optimal kinetic performances that can be expected in an imaginary set of different columns, all with different length but filled with the same support and operated at $\Delta P = \Delta P_{max}$. This prediction is based on a set of efficiency measurements conducted on a single column with fixed length. It hence needs to be ascertained that this length extrapolation is allowed and that the position of the KPL-curve in the (efficiency, time)-plane is independent of the length of the column that was used to collect the experimental data upon which it is based.

The main assumption underlying the simultaneous solution of Eqs. (7-9) is that the parameters that are contained in it are mutually independent. This implies that any data transformation based on Eqs. (7-9) is also based on the assumption that H and η are independent of the column length. When calculating a KPL-curve involving information about the retention times (which is e.g., the case when plotting the t_R-

time versus the sample based peak capacity), the effective retention factors (k) of the individual sample components should be independent of the column length as well.

Hence, one can conclude from the above that a physically valid KPL-curve can only be obtained under conditions wherein the effective H, η and k are length-independent. If satisfied, the validity then holds regardless whether an isocratic or gradient elution is being considered, since it was not needed to distinguish between both elution modes in any of the above.

In the absence of high-pressure operation effects, and provided the flow rate, the sample and the mobile phase composition remain the same, the assumption of a length-independent plate height and elution pattern is commonly accepted under isocratic conditions (see *SM*, part 2.3 for the exceptions to this condition). Under gradient conditions, it can be shown [19,22,23,30,31] (see SM, part 1.1.3 and 2.3) that the necessary and sufficient condition of a length-independent plate height and elution window is that the analytes are subjected to the same "relative mobile phase history". The latter term (in short "ϕ-history") denotes the series of ϕ-values experienced by the analytes at each given dimensionless position x' (x'=x/L) in the column. The condition of an identical relative ϕ-history also automatically guarantees that the analytes experience an identical η-history (see discussion of Eq. (S-61) in *SM*)

It can be shown (see *SM* part 1.1.2) for the case of a linear gradient that analytes will always experience the same relative mobile phase history provided the gradient steepness $\beta \cdot t_0$, the initial mobile phase ϕ_0 composition and the ratio and t_{delay}/t_0 (if any t_{delay} is present) are kept the same, regardless of the column length or the applied flow rate. The time based gradient steepness β used in this statement is usually defined as:

$$\beta = \frac{\phi_{t_{end}} - \phi_0}{t_{end} - t_{start}} = \frac{\Delta\phi}{t_G} \qquad (11)$$

whereas the delay time t_{delay} is defined as the time elapsing between the injection and the instant at which the gradient profile reaches the front of the column (note that in the general case t_{delay} is equal to the system dwell time (t_{dwell}) + any additional delay time introduced in the gradient program).

Based on expressions found in literature [19,22,32], it can also be shown that, when the analytes experience the same relative ϕ-history, also the peak compression factor G can be expected to be independent of the column length (see *SM* part 1.1.3).

As a result, it can be concluded that the length extrapolation underlying the establishment of a KPL-curve is only valid under the strict assumption that each original data point and its corresponding extrapolated data point are obtained under the same ϕ-history. For gradient elutions, this implies that, since a change in length inevitably involves a change in t_0 (flow rate is fixed during the KPL transformation), the extrapolation is only correct when t_G is adapted to keep the same $\beta \cdot t_0$ (or equivalently, t_G/t_0 constant). If the gradient program contains a delay time t_{delay} (e.g., because the system has a significant dwell volume, i.e. volume between pump and injector), the gradient programming also has to be adjusted so that the ratio t_{delay}/t_0 is kept constant, as discussed in more detail in the *SM* (Part 1.1.2). Alternatively, a delayed injection can be used to eliminate the effect of the system dwell volume (see *SM*, Part 2.3 for more details).

When ultra-high-pressure effects come into play, just keeping the same ϕ-history is no longer sufficient to ensure length-independent H-, η- and k-values (in both the isocratic and gradient mode). This is discussed in more detail in the *SM* part 2.3, where a simple correction formula that compensates for most of the error is given (Eq. S-62).

3.3 Physical interpretation of the KPM and implicit KPM-expressions

Since the data transformation underlying the KPM transforms the experimental data by keeping each measured efficiency data point together with its corresponding u_0-value, the u_0-velocity (or equivalently the flow rate F) is in fact treated as a fixed variable. This leaves the column length as the only remaining freely changeable variable that can be used to ensure that $\Delta P = \Delta P_{max}$. As can be noted by rewriting Eq. (9) and making the traditional assumption (see also *SM*, Part 2.3) that K_v and η are constants, this leads to:

$$L = \frac{K_v \cdot \Delta P}{u_0 \cdot \eta} \quad \text{and} \quad L_{max} = \frac{K_v \cdot \Delta P_{max}}{u_0 \cdot \eta} \tag{12}$$

Hence, when calculating the kinetic performance limit while keeping u_0-constant, the condition of achieving the maximal pressure simply corresponds to maximizing the column length (*SM*, Part 2.2):

$$\Delta P = \Delta P_{max} \text{ at constant } u_0 \Leftrightarrow L = L_{max} \tag{13}$$

As a consequence, it suffices to replace L by L_{max} in the expressions for N and n_p to transform a set of experimental column performance measurements into the corresponding KPL-curve. This is fully elaborated in the *SM* (Part 2.2). Table 1 summarizes the results obtained there, and provides all possible conversion expressions between the performance characteristics measured on a given column with fixed

length and the corresponding KPL-curve. As indicated, this transformation can occur using either the explicit (3rd column) or implicit (4th column) dependence on H.

A drawback of the explicit equations when used in gradient elution is that they require the calculation of a gradient plate height. Although this is perfectly possible (illustrated in the *SM*, Part 1.2), it strongly complicates things. The beauty of the implicit expressions is that they circumvent this problem, as they are directly based on the physical meaning of the KPM and hence only require the calculation of a so-called column length rescaling factor λ:

$$\lambda = \frac{\Delta P_{max}}{\Delta P_{exp}} \tag{14}$$

which is a readily obtainable experimental parameter (ΔP_{exp} is the maximum column pressure drop experienced during the gradient run conducted to measure a given N_{exp} or $n_{p,exp}$ and $t_{0,exp}$-data point, i.e. the value obtained by subtracting the extra column pressure drop). Using this λ-value, the implicit kinetic plot expressions allow to directly calculate the corresponding KPL-variables (subscript "KPL") from the experimentally measured column performance measures (subscript "exp") on a single column, via:

$$t_{0,KPL} = \lambda \cdot t_{0,exp} \tag{15}$$

$$t_{R,KPL} = \lambda \cdot t_{R,exp} \tag{16}$$

$$N_{KPL} = \lambda \cdot N_{exp} \tag{17}$$

$$n_{p,KPL} = 1 + \sqrt{\lambda} \cdot (n_{p,exp} - 1) \tag{18}$$

$$\sigma_{t,KPL} = \sqrt{\lambda} \cdot \sigma_{t,exp} \tag{19}$$

$$R_{s,i,KPL} = \sqrt{\lambda} \cdot R_{s,i,exp} \tag{20}$$

$$L_{KPL} = \lambda \cdot L_{exp} \tag{21}$$

Since every experimental data point is obtained for a different ΔP_{exp}, it is needless to say that λ is different for each measured data point, in agreement with Eq. (22) given here below. Working under conditions wherein the structural and physicochemical column parameters can be considered to be pressure-independent (see *SM*, part 2.3), it can be readily derived from Eqs. (14) and (12) that λ is inversely proportional to the mobile phase velocity u_0 or flow rate F:

$$\lambda = \frac{cst_1}{u_0} \qquad \text{or} \qquad \lambda = \frac{cst_2}{F} \tag{22}$$

3.4 Comparing different stationary phase types using the KPM

In Section 3.2, it was noted that the KPM only leads to a correct rescaling from one column length to the other provided that the analytes are subjected to the same relative ϕ-history. Considering only one type of particles (or stationary phase), this corresponds to keeping the value of $\beta \cdot t_0$, t_{delay}/t_0 and ϕ_0 constant. However, when comparing different stationary phases (which generally each have a different retention behaviour), the condition of an identical relative ϕ-history no longer suffices to keep the same elution window.

In our opinion, the best way out of this is that the comparison of different stationary phases should occur by first selecting a sample of interest, and then vary ϕ_0, ϕ_{end} and $\beta \cdot t_0$ for each phase independently until the best KPL-curve (or set of intersecting best curves) for that specific stationary phase is obtained. Performing this optimization for each stationary phase independently, one can then compare the different stationary phases, each for their own individually optimized optimum, i.e., the KPL-curve (or set of intersecting curves) lying the far most to the bottom and to the right of the time versus peak capacity plot.

In a variant to this, and assuming that the LSS-model would apply, a comparison between different phases can be achieved by keeping the same ϕ_0 and adapting β such that the same value of $S_{av} \cdot \beta \cdot t_0$ is obtained (with S_{av} the sample-averaged solvent strength parameter). This technique was illustrated by Zhang et al. [10] and allows to compare different phases in a more or less similar elution window.

4. Experimental and computational procedures

4.1 Experimental

Uracil, benzene, naphthalene, phenanthrene, methyl-, ethyl-, propyl and butylparaben were purchased from Sigma-Aldrich (Steinheim, Germany). Acetonitrile (ACN), methanol (MeOH) and water (all HPLC grade) were also purchased from Sigma-Aldrich. HALO Fused Core C_{18} columns (150 x 2.1 mm, 2.7 µm) were purchased from Advanced Materials Technologies (Wilmington, DE, USA). Zorbax Stable Bond C_{18} columns (50mm×4.6 mm, 1.8 µm; 150mm×4.6 mm, 3.5 µm and 150mm×4.6 mm, 5 µm) were purchased from Agilent Technologies (Diegem, Belgium).

For the HALO columns, all experiments were conducted in the gradient mode with an acetonitrile/water mobile phase. The initial mobile phase composition was 50%/50% (v/v) acetonitrile/water and the gradient steepness ($\beta \cdot t_0$) was kept constant during the measurement of the gradient van Deemter curves (different gradient steepness values were obtained by putting $\beta \cdot t_0$ equal to 0.008, 0.016, 0.024, 0.048

and 0.064). The initial value of ϕ and the range over which it was varied, was thus the same in each experiment, which implies that only the gradient time t_G was changed to maintain constant ratio of t_G/t_0 (or equivalently $\beta \cdot t_0$) for the different gradient steepness's. Chromatograms were recorded for at least nine different velocities on 1 column, for at least 5 velocities on the 2 coupled columns and for 3 velocities on the 4 coupled columns. The columns were tested on an Agilent 1200 HPLC system (Agilent Technologies, Waldbronn, Germany) with a diode array detector with a 1.7 µL detector cell and a binary pump. The system was operated with Agilent Chemstation software. Samples consisting of 0.02 mg/mL uracil, 0.1 mg/mL benzene, 0.05 mg/mL naphthalene and 0.05 mg/mL phenanthrene were dissolved in the initial mobile phase. The injected sample mixture volume was 1 µL. Absorbance values were measured at 210 nm with a sample rate of 80 Hz.

For the Zorbax columns, all experiments were conducted in the gradient mode with a methanol/water mobile phase. The initial mobile phase composition was 45%/55% (v/v) methanol/water and the gradient steepness ($\beta \cdot t_0$) was kept constant during the measurement of the gradient van Deemter curves ($\beta \cdot t_0$ equal to 0.020) for the different particle sizes. The columns were tested on a Dionex Ultimate 3000 system (Dionex Benelux, Amsterdam, The Netherlands) with a diode array detector with a 2.5 µL detector cell and a binary pump. The system was operated with the Dionex Chromeleon software (Dionex, Munchen, Germany). Samples consisting of 0.02 mg/mL uracil, 0.02 mg/mL methylparaben, 0.02 mg/mL ethylparaben, 0.04 mg/mL propylparaben, and 0.04 mg/mL butylparaben were dissolved in the initial mobile phase. The injected sample mixture volume was 2 µL. Absorbance values were measured at 254 nm with a sample rate of 50 Hz.

The system dwell volumes were determined using the procedure described in [33] and were determined as 450 µl for the Agilent 1200 system and 610 µl for the Dionex Ultimate 3000 system.

For every component in the chromatogram, the variances were calculated using the peak width at half height. All experiments were conducted at a temperature of 30°C. The efficiency measurements were conducted from the lowest flow rate (0.05 mL/min) up to the maximal available pressure of the instrument (600 bar) for the HALO columns. The Zorbax columns were tested from the lowest flow rate (0.062 ml/min) up to the maximal pressure allowed by the column hardware (400 bar for the 3.5 en 5µm particles and 600 bar for the 1.8µm particle column).

All reported data were obtained after correction for the system band broadening (σ^2_{ec}), t_0-time (t_{ec}) and pressure drop (ΔP_{ec}), measured by removing the column from the system and replacing it with a zero dead volume connection piece [7]:

$$\sigma^2_{col} = \sigma^2_{total} - \sigma^2_{ec} \quad (23)$$

$$t_{0,col} = t_{0,total} - t_{ec} \quad (24)$$

$$t_{R,col} = t_{R,total} - t_{ec} \quad (25)$$

$$\Delta P_{col} = \Delta P_{total} - \Delta P_{ec} \quad (26)$$

The extra column band broadening was measured for each component separately, using a mobile phase composition that resulted isocratically in the same k values as during the gradient run. The contribution of the system to the total band variance was on the HALO columns always less than 5% for phenanthrene and even smaller on the Zorbax columns. Eq. (23) however overestimates the contribution of the extra column band broadening in gradient elution, since it lumps both the pre- and post-column contributions. Whereas the latter is independent of the elution mode (isocratic or gradient), the contribution to the observed peak width of the former is much smaller in gradient elution due to the focussing effect on the front of the column (where the retention is very high at the start of the gradient). Both contributions should therefore be considered separately. Such a detailed analysis was however not performed in the present study, because the overall correction for σ^2_{ec} was anyhow small under the employed experimental conditions, except for the least retained compounds on the single column. However, for these components, the difference between the pre-column band broadening in isocratic elution and gradient elution is also limited, since the retention for the initial mobile phase composition was rather low for the least retained compounds and as a result $k(\phi_0)$ is close to the effective k as well as to k_{elut}. The corrections of t_0, t_R and ΔP are not affected by the gradient elution mode, although it should be noted that ΔP_{ec} has to be measured using the mobile phase composition that has the maximum viscosity during the gradient run.

4.2 Computational procedures

Using an in-house developed numerical integration routine (based on a fourth-order Runge–Kutta method and written in Fortran 90-code), the mass balance in a packed bed given by Eq. (27) was solved (symbols explained in the symbol list):

$$\begin{cases} \dfrac{\partial C_1}{\partial t} = -u_i \cdot \dfrac{\partial C_1}{\partial x} + D_{ax} \cdot \dfrac{\partial^2 C_1}{\partial x^2} - \dfrac{1-\varepsilon}{\varepsilon} \cdot \dfrac{\partial C_2}{\partial t} \\ \dfrac{\partial C_2}{\partial t} = \dfrac{\Lambda}{1-\varepsilon} \cdot \left(C_1 - \dfrac{C_2}{K_{eq}} \right) \end{cases} \quad (27)$$

Using either time-based moments (by monitoring the concentration profile as a function of time) at the end of the column or by calculating the spatial moments of the solute band moving through the column, values for the plate height H of the simulated packed bed were obtained. For an isocratic elution (K_{eq} is kept constant), the simulation results were in perfect agreement with the analytical solution to the problem [34]. The program also allowed to modify the inlet concentration of the mobile phase as a function of the time and thus to simulate gradient elution (K_{eq} varies with time and distance). Both LSS and non-LSS models were used to represent the variation of K_{eq} with ϕ. The accuracy of the program in the gradient elution mode was verified by checking whether the produced degrees of peak compression (see *SM* part 1.1.3 for a discussion of peak compression) under the condition of a constant H lead to the theoretical G-value predicted by Poppe et al. [32] for the LSS-case, using:

$$\ln(k_{loc}[\phi]) = \ln(k_{loc}[\phi_0]) - S\cdot(\phi-\phi_0) \qquad (28)$$

A perfect agreement was found, so that the program could subsequently be used to verify whether the KPM also works under peak compression conditions in the non-LSS case.

To mimic non-LSS conditions, Eq. (28) was modified into Eq. (29) [22,35] (for more intricate models of non-LSS behaviour, see e.g. ref. [36])

$$\ln(k_{loc}[\phi]) = \ln(k_{loc}[\phi_0]) + a_1\cdot(\phi-\phi_0) + a_2\cdot(\phi-\phi_0)^2 + a_3\cdot(\phi-\phi_0)^3 \qquad (29)$$

The time steepness of the gradient was such that $\beta\cdot t_0$ was a constant for all mobile phase velocities ($\beta\cdot t_0$ = 0.1429). Other values were: ϕ_0 = 0.5, $k_{loc}(\phi_0)$ = 15, a_1 = -10, a_2 = 7 and a_3 = -10. Simulations of the gradient elution mode under LSS-conditions were performed as well, using $k_{loc}(\phi_0)$ = 15, S = 10. The values of D_{ax} and Λ were determined using classical equations found in literature [34], using naphthalene as the model compound for its diffusion properties and using the solvent parameters of a mixture of water with ACN as organic modifier. The values of D_{ax} and Λ terms thus depended on the local mobile phase composition (via the locally varying values of η and k_{loc}). The value for ε was put at ε=0.38 and the particle size was set equal to 3.5 μm.

5. Results and discussions

All data reported below relate to gradient experiments since the validity of the kinetic plot method (KPM) has already been thoroughly investigated for the isocratic case [16,31,37]. The single exception to the possibility to use the KPM as an exact prediction tool of the performance of longer columns that was observed in these studies was when excessive viscous heating occurs in columns that behave non-adiabatic, thus inducing a length-dependent thermal effect on k and η and D_{mol}. This is however a case

wherein also the theoretical plate height concept looses its meaning as a column length-independent measure for the band broadening. In the present study, using a still air oven and either an instrument maximally delivering 600 bar or columns with the same pressure limit, such high pressure effects are still mostly insignificant [31,38].

Fig. 1 (and more precisely the full line arrow) shows the transformation of the experimentally measured peak capacity to the corresponding KPL. Using the implicit KPM, the establishment of the KPL-curve was straightforward. First, the peak capacity was determined for each considered experimental flow rate using the piece-wise mode n_p-definition given by Eq. (4). This lead to the fixed length kinetic plot curve represented by the open data symbols shown in Fig. 1. The KPL-curve was then readily obtained by using Eq. (18) and the experimentally determined set of λ-values (calculated using Eq. (14)). The approach of calculating the peak capacity using the piecewise mode of Eq. (4) is illustrated more clearly in Cabooter *et al.* [25] for the case of an isocratic separation. If preferred, the construction of both the fixed length KP and the KPL can also be based on the average peak width (i.e. by using Eqs. (5-6) instead of Eq. (4)).

Whereas Fig. 1 reports the peak capacity n_p, the expressions given in Table 1 show that it is equally well possible to plot the KPL-curve in terms of the N- or σ_t-value of an individual component, or even in terms of the R_s-value of the critical pair.

The horizontal dashed arrow represents the transformation according to the max(n_p or N) with fixed t_R-optimization (see *SM*: Part 2.1, case 1 or 2). The vertical dashed arrow represents a transformation according to the min(t_R) with fixed n_p or N-optimization (see *SM*: Part 2.1, case 3). The full line arrow corresponds to the data transformation described by Eqs. (16) and (18), i.e., by keeping u_0-constant. The transformation shown in Fig. 1 is similar to that of Fig. 2 of Eeltink et al. [39], where the physical interpretation of a kinetic plot as being the result of a column length rescaling was already given. An illustration of the data transformation from the experimentally measured gradient (H,u_0)-data to the KPL-curve is given in the *SM* (Part 2.4), also showing that the explicit KPM-expressions give the same result as the implicit expression.

The u_0=constant-transformation also constitutes the only way to preserve the experimentally determined band broadening information during a point-by-point transformation. The latter is a key feature of the kinetic plot method (KPM) [16], because it allows to treat the relation between H (or n_p or σ_t) and u_0 as

an unknown. This circumvents the need to select a plate height model and to fit this to the experimental data, as is done in the kinetic plot methods that are based on a numerical optimization routine [10,12,14,15]. Doing the transformation on a point-by-point basis, each bit of experimental band broadening information is fully preserved and does not risk to be eliminated by the fitting process. This is especially advantageous under gradient elution conditions, as there is up to date no real good model available to fit a gradient plate height curve. All newly proposed kinetic plot expressions developed in the present study rely on this point-by-point data transformation principle. The fitted curves added to the figures are only there for visualization or interpolation purposes, which have furthermore also been obtained by first fitting the experimental plate height curve and then transforming each data point of this fitted curve in a point-by-point way. The point-by-point transformation can be very easily implemented in a spreadsheet program such as Microsoft® Excel, as is illustrated in the *SM* (Part 2.4, Fig. S-4).

The key test for the validity of the KPM is that it should yield a KPL-curve that is independent of the length of the column that was used to determine the experimental data it is based on. This was verified by comparing the band broadening under gradient conditions in 3 different column lengths (resp. 1, 2 and 4 coupled columns, each with a length of 15 cm). To satisfy the conditions needed to obtain a column-length independent elution window (see *SM*, 2.3), the measurements in the different column lengths were conducted by applying the same ϕ-history, i.e., by keeping ϕ_0, t_{delay}/t_0 and $\beta \cdot t_0$ constant, implying for example that β was halved if the column length was doubled. This also corresponds to the approach adopted by Wang et al. [40] and Zhang et al. [10]. As can be noted from Fig. 2 (showing both the total sample based peak capacity as well the individual peak capacities calculated for each component separately), there is a good overlap of the KPL-data points originating from experiments conducted in columns with different length, hence providing an experimental proof for the fact that the currently proposed KPM is valid under gradient elution conditions. The agreement of the KPL-data points originating from the different length columns is equally good for the individual components and the entire sample (total n_p). Again, exactly the same KPL-curves were obtained starting using either the implicit or the explicit KPM.

Fig. 3 investigates the effect of gradient steepness on the degree of overlap of KPL-curves originating from experiments conducted in columns with different length. As can be noted, this overlap remains very good, despite the factor of 8 variation in considered gradient steepness. Similar curves were obtained for the other measured gradient steepness values, but are not shown for the sake of clarity.

Because the coupled column experiments inevitably have a limited range of velocities over which the plate height curve can be measured (the data points corresponding to the 4-column systems in Figs. 2 and 3 for example do not leave the B-term dominated regime of the plate height curves), the column length-independency of the KPL was also verified numerically, for a wide set of different parameters (see Experimental and numerical procedures). Three different columns lengths were considered (2.5, 5 and 10cm) and 8 different u_0 velocities in the range of 0.5 to 14.3 mm/s. Fig. 4 shows an example of the perfect overlap that was obtained in all investigated cases. Similar simulations using different parameters for k_0, ϕ_0, d_p and the k-dependency on ϕ all resulted in the same overlapping results (results not shown here). This perfect overlap confirms that the presently proposed KPM-expressions are independent of the length of the column wherein the experimental data were collected, even under conditions of peak compression in both LSS or non-LSS conditions. The key to this fortunate behaviour is that the conditions needed to obtain the same peak compression (i.e., keeping the same ϕ-history) are the same as those needed to keep the same elution window (see *SM*, part 1.1.3). However, deviations from the column length-independent behaviour might occur when ultra-high pressure effects occur in columns that do not behave perfectly adiabatically or isothermally, or when other length-dependent band broadening sources are present (for more detailed information: see Part 2.3 of the *SM*).

The practical use of the KPM in gradient elution is illustrated in Fig. 5, showing that the KPM can be used to evaluate what packing material (e.g. particle size or morphology) and operating conditions (e.g. temperature or gradient steepness) can deliver a desired efficiency of peak capacity in the shortest possible time [41]. This was already shown in isocratic elution to select the system the best suited to reach an efficiency of 100000 plates in a given time [37]. The effect of the system dwell volume was taken into account by keeping t_{delay}/t_0 constant in the gradient programming for the different column lengths.

Fig. 5 shows that for an operating pressure of 400 bar, and for the given gradient steepness, a peak capacity n_p of 100 is reached in shortest time (i.e. in 9.3 minutes) using 1.8µm particles, n_p = 150 using 3.5µm particles (47.4 min.) and n_p = 250 using 5µm particles (around 4.5 hours). Now extrapolating this data to an operating pressure of 1000 bar (making the assumption there would be packing materials and columns able to withstand this operating pressure), it is demonstrated that, as expected, the 1.8µm is still the best material to reach n_p = 100 (now possible in 4.9 minutes), but is now also the optimal particles choice to reach a peak capacity of 150 (in 18.9 minutes). The use of 3.5µm particles are now the best choice to reach n_p = 250 (around 2.3 hours) and 5µm particles only become advantageous for

peak capacities above n_p = 325. Considering the 1000-bar data shown in Fig. 5, it has to be noted that these are only an extrapolation and are hence prone to errors due to the influence of pressure on the physico-chemical properties of both solvent and solute [38] and the effect of viscous heating [37]. The amplitude of these effects is however limited [37,38] in adiabatic or quasi adiabatic conditions (still air oven) as were used in these experiments.

6. Conclusions

The kinetic plot method, originally developed for isocratic separations [16], has been extended to gradient elution separations by establishing a theoretical framework that allows to directly draw the kinetic performance limit (KPL) curve of a given separation medium directly from a set of measurements of the flow rate (or u_0 or the t_0-time or the t_R-time) and the separation quality (band width, band standard deviation σ_t, critical pair resolution R_s, column efficiency N, peak capacity n_p) conducted on a column with a given length. The obtained KPL-curve is valid for the sample and mobile phase conditions that were used to collect the column performance data and connects all operating points at which the tested separation medium achieves its best possible kinetic performance, i.e., achieves a given separation quality in the shortest possible time or achieves the best possible separation quality in a given time. In fact, the individual data points on the KPL-curve relate to a series of columns with a different length, but operated at the maximally available or allowable pressure, as this is the necessary and sufficient condition for a column to yield a point lying on the KPL-curve.

The established theoretical framework covers both isocratic and gradient elution conditions, and leads to either a set of explicit or a set of implicit expressions. Both approaches lead to the same KPL-curves (even if the former would be based on an inaccurate estimate of k_{elut}). The implicit expressions are however much simpler to use (cf. Eqs. (15-22)), as they are directly based on the fact that the kinetic plot method simply corresponds to a column length rescaling (cf. the use of the column length rescaling factor λ). This λ-factor needs to be determined for each individual data point on the KPL-curve. This is however a trivial exercise because λ in principle simply corresponds to the ratio of the column pressure for which the KP-curve will be established and the column pressure read-out for the flow rate for which the KPL-data point is to be calculated. As a consequence, the method can be readily implemented in any simple spread-sheet program. A possible correction to λ is needed if the viscosity of the mobile phase liquid changes with the applied pressure (because of the pressure-dependency of η and because of the viscous heating effect). In this case Eq. (S-62) (see *SM*) needs to be applied, but this is not fundamentally more difficult.

In principle, the established KPL-curve yields exact predictions of the separation performance one can expect in any column with a different length but operated at the maximal pressure, provided these different length columns are operated under the same conditions (same relative mobile phase history, same type sample components and same operating temperature) and provided the measured plate heights are not length-dependent [21,31,42]. Viscous heating effects in columns that behave perfectly adiabatic can be exactly accounted for. It is only when systems have a non-adiabatic thermal behaviour that the possibility to go from an experimental set of measurements on one column length to an exact prediction of the performance in another column length is compromised (in addition to other length dependent error sources such as extra-column band broadening or packing effects).

However, the obtained KPL-curve can even in these cases still be used as a prediction of the (virtual) performance one would obtain provided these effects would not occur. Under this assumption, the kinetic plot can still be used as a universal comparison method for the performance of differently shaped and sized support materials. If one is really after an exact prediction of the kinetic performance in systems marked by a strong viscous heating and with thermal conditions that are far from adiabatic, one will have to accept that the mathematics in these cases become so complex that the best way to establish a kinetic plot simply consists of running the actual experiments, by coupling 1,2,3, etc columns in series and test each combination at the maximal pressure, as was already done by Sandra and co-workers [43-45]. Intermediate points can then be determined via interpolation.

The present analysis has shown that the kinetic plot method remains valid under gradient elution conditions, even though the band width or peak capacity depend on the relative mobile phase history and are prone to peak compression effects. The only consequence of these effects is that the established KPL-curve is only valid provided ϕ_0, the gradient steepness $\beta \cdot t_0$ and t_{delay}/t_0 are maintained constant when the column length is changed. This implies for example that β needs to be halved if the column length is doubled. This condition holds for LSS as well as for non-LSS systems. Although the present study and analysis only considered linear gradient systems, it can be inferred that the general rule concerning the requirement of a constant relative mobile phase history will also hold for non-linear gradients. Special effects such as organic modifier retention or large changes in k_{loc} across the peak width on the validity of the kinetic plot extrapolation will be investigated in a future study.

As was shown in a practical example, the KPM can now be readily used to determine the best possible particle size to produce a given peak capacity in the shortest time under gradient elution for a fixed gradient steepness.

Supplementary material

Supplementary material (SM) available: This material is available alongside the electronic version of this article.

Acknowledgement:

K.B. and D. Ca. gratefully acknowledge a research grant from the Research Foundation – Flanders (FWO Vlaanderen).

References:

[1] A.D. Jerkovich, J.S. Mellors, J.W. Jorgenson, J.W. Thompson, Anal. Chem. 77 (2005) 6292.
[2] K.D. Patel, A.D. Jerkovich, J.C. Link, J.W. Jorgenson, Anal. Chem., 76 (2004) 5777.
[3] H. Chen, Cs. Horvath, J. Chromatogr. A, 705 (1995) 3-20.
[4] J. Thompson, P. Carr, Anal. Chem., 74 (2002) 1017.
[5] B. Yan, J. Zhao, J.S. Brown, J. Blackwell, P. Carr, Anal. Chem., 72 (2000) 1253-1262.
[6] F. Lestremau, A. Cooper, R. Szucs, F. David, P. Sandra, J. Chromatogr. A, 1109 (2006) 191-196.
[7] D. Guillarme, S. Heinisch, J.-L. Rocca, J. Chromatogr. A, 1052 (2004) 39-51.
[8] N. Tanaka, H. Kobayashi, K. Nakanishi, H. Minakuchi, N. Ishizuka, Anal. Chem., 73 (2001) 420-429.
[9] F. Svec, LC·GC Europe, 16 (6a) (2003) 24-28.
[10] Y. Zhang, X. Wang, P. Mukherjee, P. Petersson, J. Chromatogr. A, 1216 (2009) 4597–4605.
[11] J.C. Giddings, Anal. Chem., 37 (1965) 60-63.
[12] J.H. Knox, M. Saleem, J. Chromatogr. Sci. 7 (1969) 614-622.
[13] G. Guiochon, Anal. Chem., 53 (1981) 1318-1325.
[14] H. Poppe, J. Chromatogr. A, 778 (1997) 3-21.
[15] X. Wang, D.R. Stoll, P.W. Carr, P.J. Schoenmakers, J. Chromatogr. A, 1125 (2006) 177–181.
[16] G. Desmet, D. Clicq, P. Gzil, Anal. Chem., 77 (2005) 4058-4070.
[17] T. Hara, I. Kobayashi, K. Nakanishi, N. Tanaka, Anal. Chem., 78 (2006) 7632-7640.
[18] D. Guillarme, E. Grata, G. Glauser, J.-L. Wolfender, J.-L. Veuthey, S. Rudaz, J.Chromatogr. A, 1216 (2009) 3232-3243.

[19] L.R. Snyder, D.L. Saunders, J. Chromatogr. Sci., 7 (1969) 195-208.
[20] L.R. Snyder, J.W. Dolan, J.R. Gant, J. Chromatogr., 165 (1979) 3-30.
[21] G. Guiochon, Chromatogr. A, 1126 (2006) 6–49.
[22] F. Gritti, G. Guiochon, J. Chromatogr. A, 1145 (2007) 67–82.
[23] U.D. Neue, J. Chromatogr. A, 1079 (2005) 153–161.
[24] U.D. Neue, J. Chromatogr. A 1184 (2008) 107–130.
[25] D. Cabooter, A. de Villiers, D. Clicq, R. Szucs, P. Sandra, G. Desmet, J. Chromatogr. A, 1147 (2007) 183.
[26] J.C. Giddings, Anal. Chem., 39 (1967) 1027-1028.
[27] M. Gilar, U.D. Neue, J. Chromatogr. A., 1169 (2007) 139–150.
[28] S. Eeltink, S. Dolman, R. Swart, M. Ursem, P.J. Schoenmakers, J. Chromatogr. A, 1216 (2009) 7368-7374.
[29] J. Cazes, R.P.W. Scott, Chromatography theory, Marcel Dekker Inc: New York, 2002.
[30] U.D. Neue HPLC-Columns—Theory, Technology, and Practice; Wiley-VCH: Weinheim, 1997.
[31] D. Cabooter, F. Lestremau, A. de Villiers, K. Broeckhoven, F. Lynen, P. Sandra, G. Desmet, J. Chromatogr. A, 1216 (2009) 3895-3903.
[32] H. Poppe, J. Paanakker, M. Bronckhorst, J. Chromatogr., 204 (1981) 77–84.
[33] L. R. Snyder, J. W. Dolan., High Performance Gradient Elution, The practical application of the linear-solvent-strength model, Wiley-Interscience: Hoboken, New Jersey, USA, 2007.
[34] G. Desmet, K. Broeckhoven, Anal. Chem., 80 (2008) 8076–8088.
[35] F. Gritti, G. Guiochon, J. Chromatogr. A, 1212 (2008) 35–40.
[36] U. D. Neue, Chromatographia, 63 (2006) S45-S53.
[37] D. Cabooter, F. Lestremau, F. Lynen, P. Sandra, G. Desmet, J. Chromatogr. A, 1212 (2008) 23-34.
[38] U.D. Neue, M. Kele, J. Chromatogr. A, 1149 (2007) 236-244.
[39] S. Eeltink, G. Desmet, G. Vivo-Truyols, G. Rozing, P.J. Schoenmakers, W.Th. Kok, J. Chromatogr. A 1104 (2006) 256-262.
[40] X. Wang, W.E. Barber, P.W. Carr, J. Chromatogr. A, 1107 (2006) 139-151.
[41] P.W. Carr, X. Wang, D.R. Stoll, Anal. Chem., 81 (2009) 5342-5353.
[42] K. Broeckhoven, G. Desmet, J. Chromatogr. A, 1216 (2009) 1325–1337.
[43] F. Lestremau, A. Cooper, R. Szucs, F. David, P. Sandra, J. Chromatogr. A, 1109 (2006) 191-196.
[44] A. de Villiers, F. Lestremau, R. Szucs, S. Gélébart, F. David, P. Sandra, J. Chromatogr. A, 1127 (2006) 60-69.
[45] F. Lestremau, A. de Villiers, F. Lynen, A. Cooper, R. Szucs, P. Sandra, J. Chromatogr. A, 1138 (2007) 120-131.

List of symbols:

cst	constant, [m/s] or [m³/s]
C_1	concentration in the mobile phase, [mol/m³]
C_2	concentration in the stationary phase, [mol/m³]
D_{ax}	lumped axial dispersion coefficient (both A and B-term contribution), [m²/s]
i	i-th elution component, [/]
F	flow rate, [m³/s]
H	plate height, see Eq. (1), [m]
k	phase retention factor, defined as $(t_R-t_0)/t_0$, [/]
k_{elut}	effective phase retention factor at point of elution, [/]
k_{loc}	local phase retention factor, [/]
K_v	permeability, based on u_0, [m²]
K_{eq}	whole particle based equilibrium constant [34], [/]
L	column length, [m]
n	number of components in sample, [/]
N	actual column plate count [/], see Eq. (1), [/]
N_{eff}	effective plate number, defined as $N_{eff} = N \cdot k^2/(1+k)^2$, [/]
n_p	peak capacity, [/]
$R_{s,i}$	separation resolution of peaks i-1 and i, also see Eq. (S-57) in the *SM*, [/]
S	linear solvent strength parameter, see Eq. (28), [/]
t	time, [/]
t_0	column residence time for an unretained marker (k=0), [s]
t_R	column residence time for an retained component, [s]
u_0	unretained species velocity, [m/s]
u_i	interstitial velocity, [m/s]
w	peak width, defined as $4 \cdot \sigma_t$, [s]
x	actual axial position or coordinate in column, [m]
x'	dimensionless axial position, x/L [/]
ΔP	pressure drop, [Pa]

Greek symbols:

β	time steepness of the gradient, see Eq. (11), [1/s]
ε	external porosity, [/]

ϕ	fraction of organic modifier in mobile phase composition, [/]
ϕ_0	fraction of organic modifier at the start of the gradient run, [/]
η	dynamic fluid viscosity, [$kg \cdot m^{-1} \cdot s^{-1}$]
λ	column length rescaling factor, see Eq. (14), [/]
Λ	lumped mass transfer coefficient, denoted as λ in ref. [34], [1/s]
σ_t	time-based standard deviation of a species band, [s]
σ_x^2	spatial variance of a species band, [m²]
σ_t^2	time-based variance of a species band, [s²]

Subscripts:

col	column contribution to band broadening and pressure drop
ec	extra column, denoting system contributions to band broadening and pressure drop
elut	conditions at end of column at moment of elution of the component
end	end of the gradient run
exp	experimentally measured
i	component index number
KPL	kinetic plot or kinetic performance limit, denoting the condition at which a given u_0 is obtained in a column operating at maximum system pressure drop
loc	local value (i.e., value at given x)
max	maximum, at maximum system pressure drop
n	number or eluting compounds = index number for last eluting component
start	start of the gradient run
total	extra column + column contribution

Figure Captions

Figure 1. Data transformation according to the implicit kinetic plot expression (Eq. (18)), starting from the measured sample peak capacity (fixed length kinetic plot, open symbols) and transforming it into its corresponding kinetic performance limit for ΔP_{max} = 600 bar (free length kinetic plot, full symbols). The meaning of the arrows is given in the text. Experimental conditions: gradient elution (ACN/H_2O) with ϕ_0 = 0.5 and $\beta \cdot t_0$ = 0.016 on a single (15cm) HALO column. Please note that different u_0-data points are obtained with a different β, so as to keep a constant $\beta \cdot t_0$.

Figure 2. Verification of the overlap of KPL-curves that originate from experiments conducted in columns with different length for the three different components (open symbols; benzene: green curve, naphthalene: red curve, phenanthrene: black curve) and the three considered column lengths (15 cm: ◊; 30cm: Δ; 60cm: □). In addition, the KPL for the total peak capacity (full symbols; blue curve, calculated by Eq. (14) and (18)) has been given as well.

Figure 3. Verification of the overlap of the KPL curves originating from experiments conducted in columns with different length (15 cm: ◊; 30cm: Δ; 60cm: □) for various degrees of gradient steepness ($\beta \cdot t_0$ = 0.008, 0.016 and 0.064). Please note that β was changed inversely proportional to L in order to keep the same $\beta \cdot t_0$ and that the gradient programming was adapted to ensure a constant t_{delay}/t_0.

Figure 4. KPL-curves based on the numerical simulation of the migration of a component (with the diffusion properties of naphthalene) through columns with different lengths in gradient elution (2.5 cm: ◊; 5cm: Δ; 10cm: □). The black curves denote a component with non-LSS behavior, the green curve denotes one with LSS behavior.

Figure 5. KPL-curves for 3 different particle sizes (5µm: ■, 3.5µm ♦ and 1.8µm ▲) in gradient elution (MeOH/H_2O) with ϕ_0 = 0.45 and $\beta \cdot t_0$ = 0.020 of the paraben mixture on the Zorbax columns. Full curves and symbols denote ΔP_{max} = 400 bar, dashed curves and open symbols denote an extrapolation to ΔP_{max} = 1000 bar.

Table 1: Most important expressions describing the relation between the experimentally determined kinetic column performance parameters and the kinetic performance limit values (denoted with subscript KPL).

Experimental Column Performance Parameters		**Kinetic Performance Limit Parameters**	
Directly measurable parameters	Calculated parameters	Explicit expressions	Implicit expressions
	$N_i = N_{meas,i} \cdot \frac{(1+k_{elut,i})^2}{(1+k_i)^2}$	$t_{0,KPL} = \frac{\Delta P_{max} \cdot K_v}{u_0^2 \cdot \eta}$	$t_{0,KP} = \lambda \cdot t_{0,exp}$
		$t_{R,KPL} = t_{0,KPL}(1+k)$	$t_{R,KP} = \lambda \cdot t_{R,exp}$
u_0 or F	$H_i = \frac{L_{exp}}{N_i}$	$N_{i,KPL} = \frac{\Delta P_{max} \cdot K_v}{u_0 \cdot \eta} \cdot \frac{1}{H}$	$N_{i,KPL} = \lambda \cdot N_{i,exp}$
$N_{meas,i}$	$n_p = 1 + \sum_{i=1}^{n} \frac{t_{R,i} - t_{R,i-1}}{4 \cdot \sigma_{t,i}}$		
	$= 1 + \frac{1}{4} \sum_{i=1}^{n} \sqrt{N_{i,meas}} \cdot \frac{k_i - k_{i-1}}{1+k_i}$	$\sigma_{t,i,KPL} = \frac{1+k'_{elution}}{u_0} \cdot \sqrt{\frac{H_i \cdot \Delta P_{max} \cdot K_v}{u_0 \cdot \eta}}$	$\sigma_{t,i,KP} = \cdot\sqrt{\lambda} \cdot \sigma_{t,i,exp}$
t_0, $t_{R,i}$		$n_{p,KPL} = 1 + \frac{1}{4} \sum_{i=1}^{n} \sqrt{\frac{\Delta P_{max} \cdot K_v}{u_0 \cdot \eta \cdot H_i}} \cdot \frac{k_i - k_{i-1}}{1+k_{elut,i}}$	$n_{p,KP} = 1 + \sqrt{\lambda} \cdot (n_{p,exp} - 1)$
ΔP or K_v	$R_s = \frac{t_{R,i} - t_{R,i-1}}{4 \cdot \frac{(\sigma_{t,i} + \sigma_{t,i-1})}{2}}$	$R_{s,KPL} = \frac{1}{2} \cdot \sqrt{\frac{\Delta P_{max} \cdot K_v}{u_0 \cdot \eta}} \cdot$	
$\sigma_{t,i}$	$= \frac{1}{2} \cdot \frac{k_i - k_{i-1}}{\frac{(1+k_i)}{\sqrt{N_{i,meas}}} + \frac{(1+k_{i-1})}{\sqrt{N_{i-1,,meas}}}}$	$\frac{k_i - k_{i-1}}{\sqrt{H_i} \cdot (1+k_{elut,i}) + \sqrt{H_{i-1}} \cdot (1+k_{elut,i-1})}$	$R_{s,KPL} = \sqrt{\lambda} \cdot R_{s,exp}$

(*) under isocratic elution conditions: $k_{elut} = k$

Figure 1

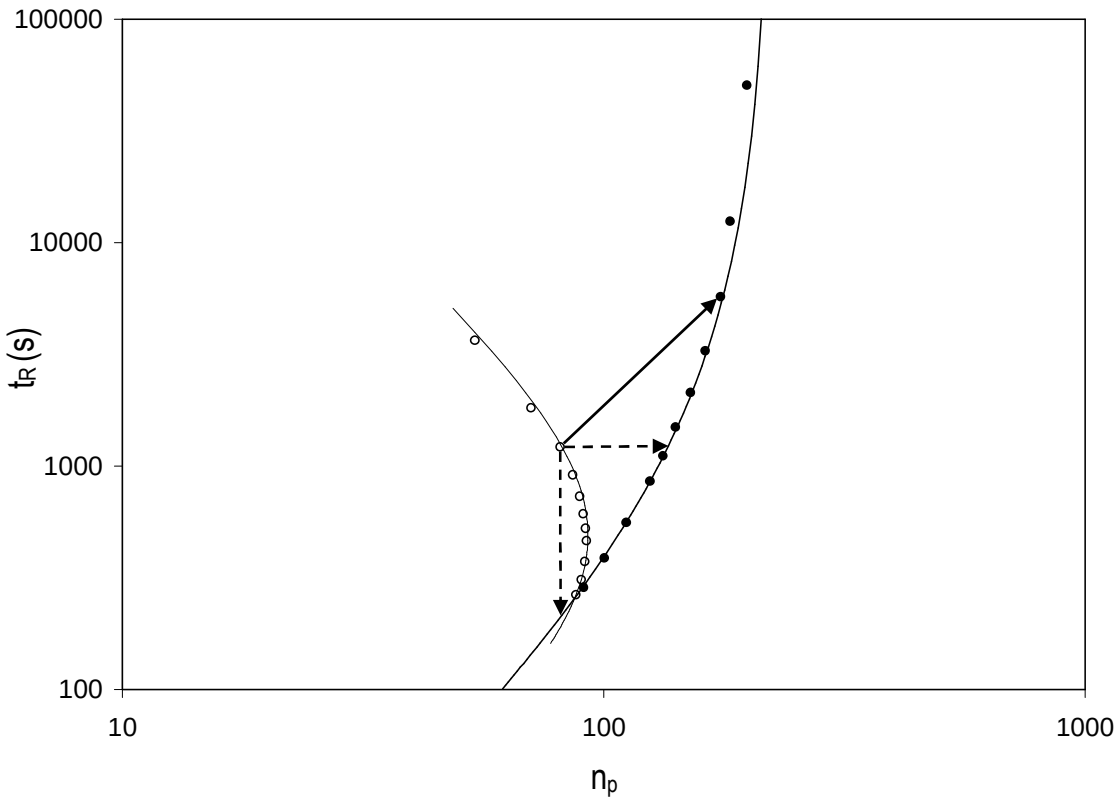

Figure 2

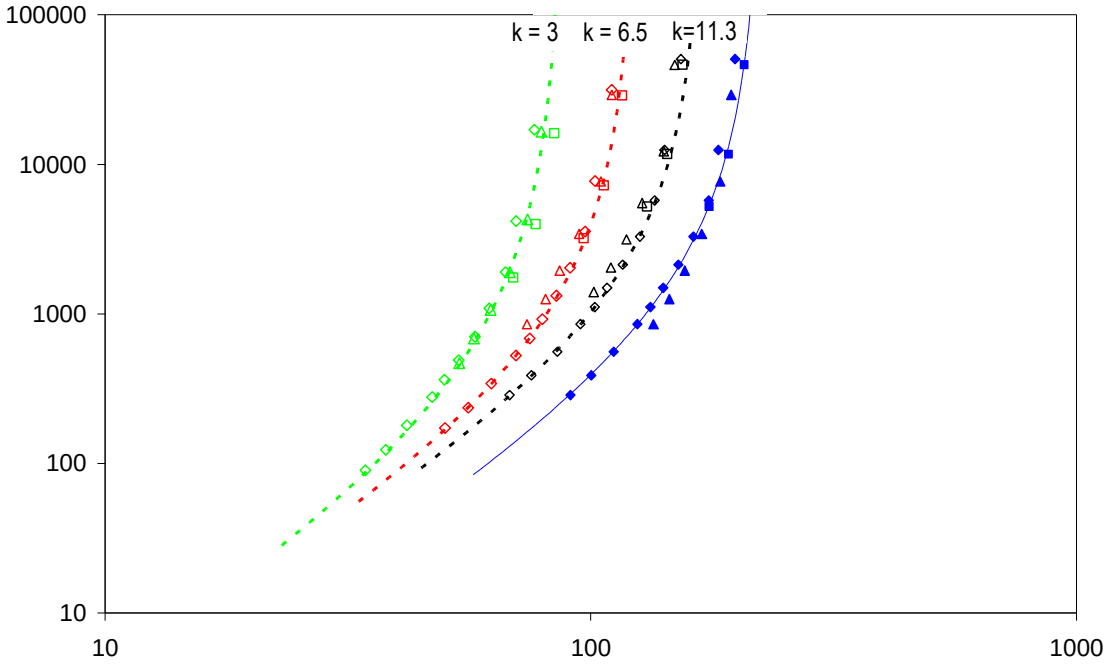

Figure 3

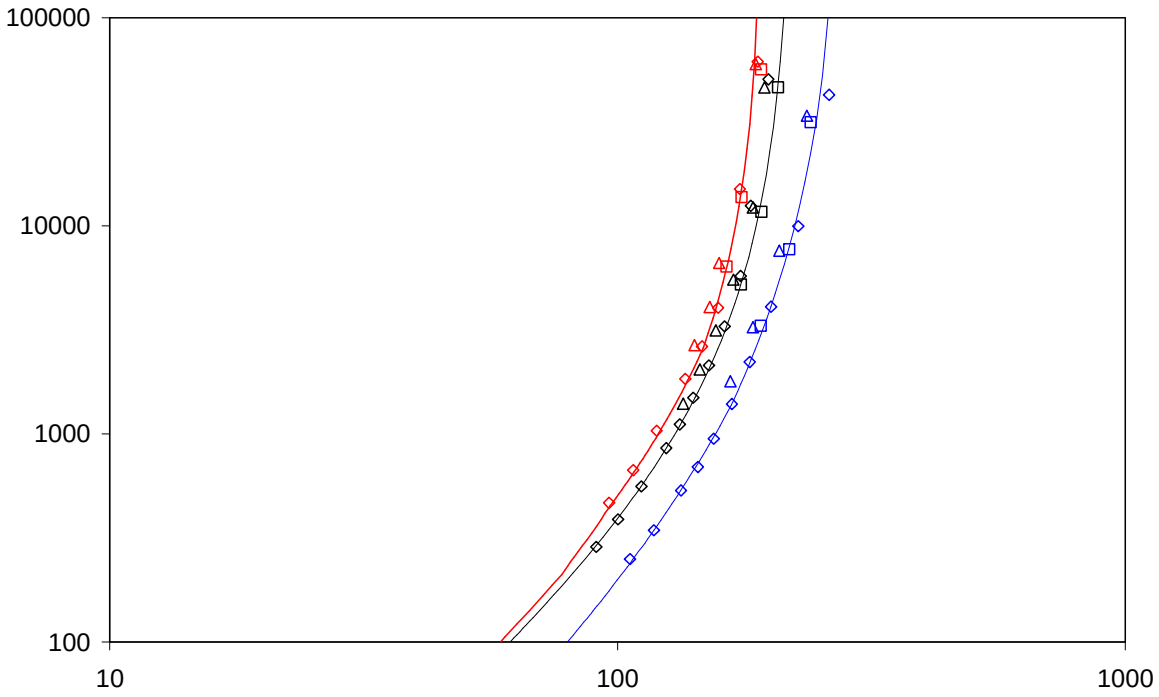

Figure 4

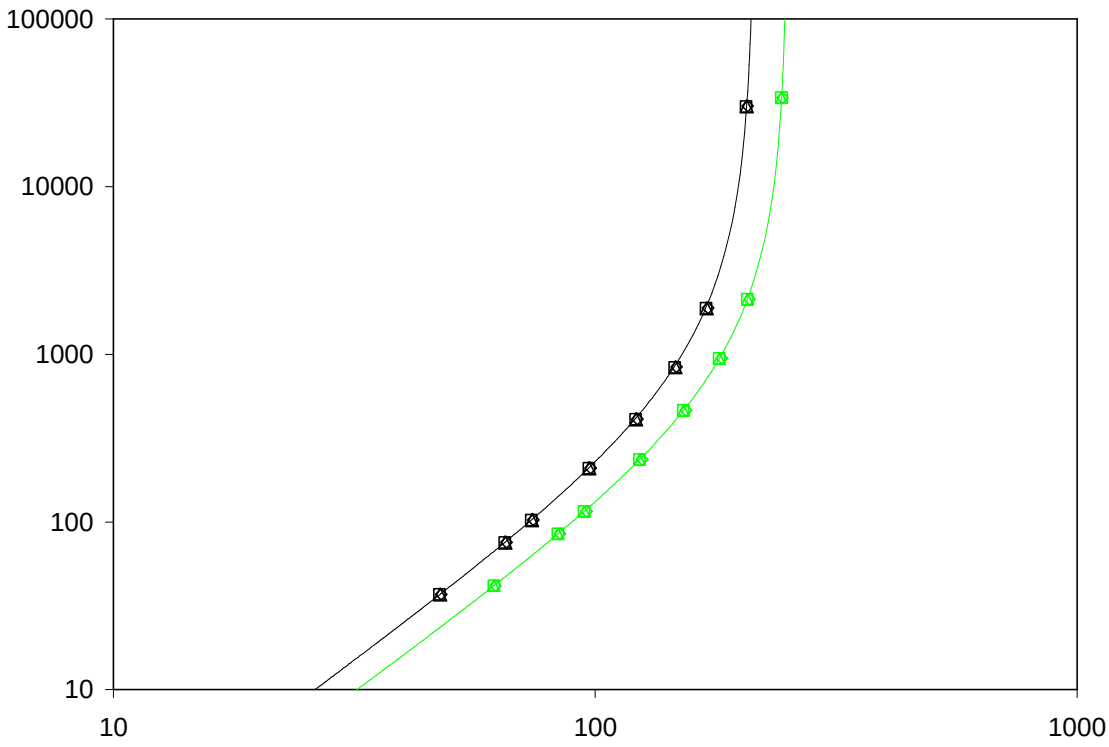

Figure 5

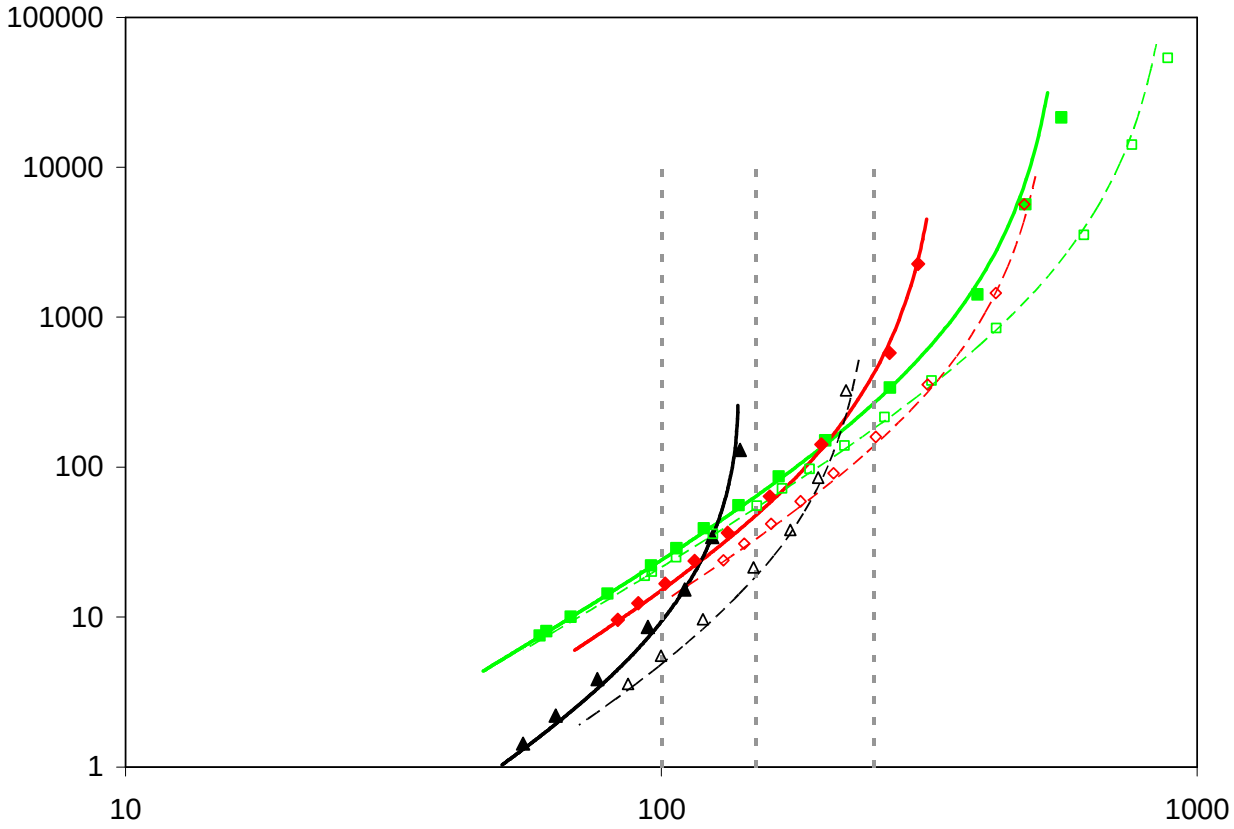

Supplementary Material

The kinetic plot method applied to gradient chromatography: theoretical framework and experimental validation

K. Broeckhoven[1], D. Cabooter[1], F. Lynen[2], P. Sandra[2] and G. Desmet[1,*]

(1) *Vrije Universiteit Brussel, Department of Chemical Engineering, Pleinlaan 2, 1050 Brussels, Belgium*
(2) *Dept. of Organic Chemistry, Universiteit Gent, Krijgslaan 281 S4-Bis, 9000 Gent, Belgium*

Abstract

The present supplementary material contains a section on the background theory of column performance in isocratic and gradient elution and the description of the gradient plate height concept (Part 1). In addition, the concept of a constant "relative mobile phase history" is introduced, which is necessary to define a gradient plate height and to apply the kinetic plot method (KPM) in gradient elution. Experimental results illustrating the use of the gradient plate height concept are given as well.

Part 2 gives a detailed derivation of the conditions needed to operate at the kinetic performance limit (KPL), i.e. the conditions needed to achieve a given N or n_p in the shortest possible time t_R, or, equivalently, to achieve a maximal N or n_p in a given time t_R (Problem 1). It is also shown that calculating the KPL on the basis of a set of experimentally measured column performance data should best be done via a data transformation that leaves the u_0-velocity corresponding to each data point invariant, and that this can be done very simply by introducing a column length rescaling factor (Problem 2)., In addition, it is investigated under which conditions the kinetic performance limit curve is independent of the length of the column in which the experimental column performance data were obtained (Problem 3). Finally, the transformations underlying the kinetic plot method (KPM) are illustrated and visualized.

Table of contents

Part 1: Background theory on column performance and plate height in gradient elution

1.1) Theory on column performance in gradient elution

1.1.1) Relation between the existing column efficiency measures

The main difficulty with the use of plate heights and plate numbers under gradient elution conditions is that it can not be determined directly from the experimental gradient data because the observed time-based width of the peaks (expressed here in terms of the observed standard deviation σ_t) is related to the retention factor at the moment of elution (k_{elut}) and not to the observed or effective retention factor k (i.e., that based on the observed retention time and defined as $k=(t_R-t_0)/t_0$) [S1-S3]:

$$\sigma_t = \frac{1}{\sqrt{N}} \cdot t_0.(1+k_{elut}) \qquad \text{(S-1)}$$

As a consequence, and noting that k_{elut} is always smaller than k in gradient elution, the bands eluting from the column appear to have broadened much less strongly than under isocratic conditions, for which:

$$\sigma_t = \frac{1}{\sqrt{N}} \cdot t_0.(1+k) \qquad \text{(S-2)}$$

The reader should note that the N in Eq. (S-1) and that in Eq. (S-2) both relate to the spatial width occupied by the bands in the column, in agreement with the basic definition of column efficiency (see Eqs. (S-4-S-5) further on). However, the N used in Eq. (S-2) (isocratic conditions) generally has a different value than that used in Eq. (S-1) (gradient conditions), due to typical gradient elution effects such as the peak compression effect or the effect of the changing mobile phase conditions on the band broadening (as discussed further on). To avoid confusion with existing notation in literature [S1,S2,S4], it should also be noted that the N in Eq. (S-1) already incorporates these effects, hence the absence of a peak compression factor G [S1,S5,S6] in Eq. (S-1).

Under gradient elution conditions, the N used in Eqs. (S-1-S-2) is also different from the plate number N_{meas} that is reported by the data analysis software accompanying commercial HPLC instruments [S1,S2] and defined as:

$$N_{meas} = \frac{t_R^{\,2}}{\sigma_t^2}, \qquad \text{(S-3)}$$

The problem with N_{meas} is that it increases too strongly with the retention time of the components to be representative of the column performance measure [S2]. A visual inspection of Eq. (S-3) readily shows this: t_R increases linearly with k, while the width of the peaks (represented by σ_t in Eq. (S-3)) only

increases according to the much smaller k_{elut}. Since furthermore the difference between k and k_{elut} grows with increasing k, the value of N_{meas} continuously increases with increasing k, hence suggesting the column quality improves with increasing residence time of the employed components. The N_{meas}-value therefore is a futile column performance measure and provides no direct information on the true column efficiency, i.e., that related to the spatial width occupied by the bands in the column. To show that this "true" efficiency corresponds to the N-value already defined in Eq. (S-1), it is instructive to start from the well-established relation [S2]:

$$\sigma_x^{\,2} = \sigma_t^{\,2} \cdot u_{elut}^{\,2} = \sigma_t^{\,2} \cdot \left(\frac{u_0}{1+k_{elut}} \right)^2 \qquad \text{(S-4)}$$

wherein σ_x^2 is the spatial variance of the band, σ_t^2 is the time-based variance of the band, u_0 the velocity of an unretained marker and u_{elut} the retained species velocity at the point of elution ($u_{elut}=u_0/[1+k_{elut}]$). Using now the well-established relationship between N and the spatial variance ($N=L^2/\sigma_x^2$), Eq. (S-4) can be transformed into:

$$N = \frac{L^2}{\sigma_x^2} = \frac{t_0^{\,2}}{\sigma_t^2} \cdot (1+k_{elut})^2 \qquad \text{(S-5)}$$

which can readily be rewritten into the expression given in Eq. (S-1).

As already mentioned, the true gradient N is seldom used because it can only be calculated from N_{meas} provided the value of k_{elut} is known, as can readily be seen after combining Eqs. (S-3) and (S-5)):

$$N = N_{meas} \cdot \frac{(1+k_{elut})^2}{(1+k)^2} = \frac{t_R^{\,2}}{\sigma_t^2} \cdot \frac{(1+k_{elut})^2}{(1+k)^2} \qquad \text{(S-6)}$$

If the linear solvent strength (LSS)-model [S1,S7] (see Eq. S-19 or Eq. 28 in main article) applies, the relation between k_{elut} and k can be predicted, so that the unknown k_{elut} on the right hand side of Eq. (S-6) can be expressed in terms of k:

$$N = N_{meas} \cdot \frac{\left(1+\frac{e^{k \cdot S \cdot \beta \cdot t_0} - 1}{S \cdot \beta \cdot t_0 \cdot e^{S \cdot \beta \cdot t_0 \cdot k}} \right)^2}{(1+k)^2} = \frac{t_R^{\,2}}{\sigma_t^2} \cdot \frac{\left(1+\frac{e^{k \cdot S \cdot \beta \cdot t_0} - 1}{S \cdot \beta \cdot t_0 \cdot e^{S \cdot \beta \cdot t_0 \cdot k}} \right)^2}{(1+k)^2} \qquad \text{(S-7)}$$

wherein S is the linear solvent strength parameter of a given component (see Eq. (S-19) further on) and β the time steepness of the gradient ($\beta=[\phi_{tend}-\phi_0]/[t_{end}-t_{start}]$). Eq. (S-7) is only valid if the dwell volume of the system is small compared to the column dead time or if the value of k at the initial mobile phase

composition is large. In the latter case Eq. (S-7) can further be simplified as shown in [S7]. In addition, as has been reported numerous times, the linear solvent strength (LSS) assumption might lead to important errors on the value of k_{elut} [S4,S8-S10]. The value of k_{elut} can also be calculated using numerical procedures [S5] or by measuring the value of k in isocratic elution with the mobile phase composition ϕ_{elut} at which the component elutes during the gradient, because ϕ_{elut} can in principle be directly calculated from the gradient parameters ϕ_0 and β. Determining ϕ_{elut} is however also prone to errors, since it involves accurately determining the system dwell volume, the column dead time and the possible retention of the organic modifier [S5]. Under isocratic conditions, there is no need to distinguish between the true and the measured plate number, for in this case $k=k_{elut}$, so that the second factor on the right hand side of Eqs. (S-6) and (S-7) becomes unity.

1.1.2) Conditions to keep the elution pattern independent of the column length

Keeping the same stationary phase and gradient time, but changing the length of the column or the applied flow rate usually leads to a change of the retention factor of the analytes under gradient elution. This is a complication which does not exist in isocratic elution and makes the kinetic optimization of gradient separations more difficult. The present section is concerned with finding the necessary and sufficient conditions to maintain the same effective retention factor k when L and F are changed.

Starting from the generally accepted ergodic process assumption and the definition of the local retention time in chromatography, it can be written that [S5]:

$$\frac{dt_s}{k_{loc}} = dt_m \qquad \text{(S-8)}$$

In case of a linear gradient with delay time t_{delay} (with t_{delay} the time elapsing between the injection and the instant at which the gradient profile reaches the front of the column; note that in the general case t_{delay} is equal to t_{dwell} + any additional delay time introduced in the gradient program), the solvent composition at any point or time in the column is given by:

$$\phi(x,t) = \phi_0 \qquad (\text{for } t<t_{delay}+x/u_0) \qquad \text{(S-9a)}$$

$$\phi(x,t) = \phi_0 + \beta\cdot(t - t_{delay} - x/u_0) \qquad (\text{for } t>t_{delay}+x/u_0) \qquad \text{(S-9b)}$$

Since for any position x we can state that the time spent in the stationary phase is equal to the total time minus the time needed for the mobile phase to reach that distance, we have $t_s=t-x/u_0$, so that Eqs. (S-9a-b) become:

$$\phi(t_s) = \phi_0 \qquad \text{for } t_s<t_{delay} \qquad \text{(S-10a)}$$

$$\phi(t_s) = \phi_0 + \beta \cdot (t_s - t_{delay}) \qquad \text{for } t_s>t_{delay} \qquad \text{(S-10b)}$$

Integrating now Eq. (S-8), and splitting the left hand side integral in two pieces, one for the constant ϕ-part, and one for the linear gradient part, we obtain:

$$\int_0^{t_R - t_0} \frac{dt_s}{k_{loc}} = \int_0^{t_0} dt_m = t_0 \qquad \text{(S-11)}$$

$$\int_0^{t_{delay}} \frac{dt_s}{k_{loc}(\phi_0)} + \int_{t_{delay}}^{t_R - t_0} \frac{dt_s}{k_{loc}(\phi_0 + \beta(t_s - t_{delay}))} = \int_0^{t_0} dt_m = t_0 \qquad \text{(S-12)}$$

Introducing subsequently the dimensionless time $t'=t_s/t_0$, the ϕ-history can be rewritten as:

$$\phi(t') = \phi_0 \qquad \text{for } t'<t_{delay}/t_0 \qquad \text{(S-13a)}$$

$$\phi(t') = \phi_0 + \beta t_0 \cdot (t' - t_{delay}/t_0) \qquad \text{for } t'>t_{delay}/t_0 \qquad \text{(S-13b)}$$

while Eq. (S-12) becomes:

$$\int_0^{t_{delay}/t_0} \frac{dt'}{k_{loc}(\phi_0)} + \int_{t_{delay}/t_0}^{(t_R - t_0)/t_0} \frac{dt'}{k_{loc}(\phi_0 + \beta t_0 (t' - t_{delay}/t_0))} = 1 \qquad \text{(S-14)}$$

Introducing an effective retention factor k as $k=(t_R-t_0)/t_0$, as done in the present study, it follows readily from Eq. (S-14) that k (appearing in the upper boundary of the integral in the second term on the left hand side) will be independent of the column length provided the ϕ_0, the product βt_0 and the ratio of t_{delay}/t_0 are kept constant

From this observation, one can directly conclude that, if any change in L or F (both inevitably leading to a change of t_0) is accompanied by a change of t_G and t_{delay} such that βt_0 and t_{delay}/t_0 are kept constant, it is guaranteed that the same elution profile (i.e., same k-values) will be obtained. This of course only holds

provided the retention properties of the stationary phase are independent of L, but this is in most cases a reasonable assumption.

At this point, it is convenient to introduce the term "relative mobile phase-history" (in short "ϕ-history") to denote the change of ϕ experienced by the components at each given dimensionless position x' (x'=x/L) in the column. This can be done by noting that $dt_m=dx/u_0 = dx.(t_0/L)=t_0.dx'$. Using this identity in Eq. (S-8), and introducing now the symbol k(x) to denote the average retention factor experienced by a component up to a given position x in the column, we can use the identity $k(x)=t_s(x)/(x/u_0)$ to obtain:

$$k(x') = t'(x') / x' \qquad \text{(S-15)}$$

on the one hand, and

$$k(x') = \frac{1}{x'} \int_0^{x'} k_{loc}(x')dx' \qquad \text{(S-16)}$$

on the other hand. Eq. (S-13) then becomes:

$$\phi(x') = \phi_0 \qquad \text{for } x' < t_{delay}/(k_{loc}(\phi_0).t_0) \qquad \text{(S-17a)}$$

$$\phi(x') = \phi_0 + \beta t_0 \cdot (k(x').x' - t_{delay}/t_0) \qquad \text{for } x' > t_{delay}/(k_{loc}(\phi_0).t_0) \qquad \text{(S-17b)}$$

Although Eqs (S-16) and (S-17) are not directly analytically solvable (the solution requires an iterative numerical procedure), their combination can be used to show that linear gradients run with the same gradient steepness $\beta \cdot t_0$ and with the same ϕ_0 and t_{delay}/t_0 are guaranteed to subject the sample components to the same ϕ-value when reaching the same dimensionless position x' (x'=x/L) in the column, regardless of the value of F or L.

As noted by one reviewer, t_{delay} can easily be removed from the problem for the case wherein t_{delay} is only determined by the dwell time. In this case, it suffices to introduce an injection delay time that exactly counters the value of t_{dwell}. When some of the t_{delay} is an essential part of the gradient program this is no longer possible.

1.1.3) Necessary conditions to keep the plate height independent of the column length

Putting forward that the plate height concept only becomes a useful tool for the analysis and the kinetic optimization of a given support type when it is length-independent, the present section studies the conditions that are needed to obtain a length-independent H-value when using the general definition of:

$$H = \frac{L}{N} \qquad \text{(S-18)}$$

with N given by Eq. (S-5). For isocratic elution, the use of this defintion is rather straightforward, but for gradient elution this is more complex.

Apart from the problematic measurement of N (see Section 1.1.1), another reason for the reluctance towards the use of plate numbers or plate heights in gradient elution is that the plate height continuously varies during the separation due to the changes in both diffusion coefficient and retention factor complementing the continuous change in mobile phase composition. Whereas the relation between D_{mol} and ϕ is complex and therefore difficult to express, the relation between ϕ and the local retention coefficient k_{loc} is usually better known. For example, when the LSS model applies, this relation can be written as [S1]:

$$k_{loc}(\phi) = k_{loc}(\phi_0) \cdot e^{-S\cdot(\phi-\phi_0)} \qquad \text{(S-19)}$$

Despite the fact that k_{loc} and D_{mol} continuously change with the position in the column under gradient elution conditions, it nevertheless remains perfectly possible to define a local plate height, H_{loc}, as well as a global plate height H. Taking the definition of the local plate height [S11], and adopting a general form of the van Deemter equation to express the dependency of H_{loc} on the mobile phase velocity u, it is always possible to put [S7]:

$$H_{loc} = \frac{d\sigma_x^{\,2}}{dx} = A(u_0, D_{mol}) + \frac{B(k_{loc}, D_{mol})}{u_0} + C(k_{loc}, D_{mol}) \cdot u_0 \qquad \text{(S-20)}$$

Since k and D_{mol} depend in a deterministic way upon ϕ, we can also write:

$$H_{loc}(\phi) = \frac{d\sigma_x^{\,2}}{dx} = A(u_0, \phi) + \frac{B(\phi)}{u_0} + C(\phi) \cdot u_0 \qquad \text{(S-21)}$$

Since the gradient operation also imposes a deterministic relation between the ϕ-value experienced by the analytes at a given dimensionless axial position x' (x'=x/L) in the column, Eq. (S-21) can be rewritten as:

$$H_{loc}(x') = A(u_0, x') + \frac{B(x')}{u_0} + C(x') \cdot u_0 \qquad \text{(S-22)}$$

To calculate the total variance of a peak in a column, the local plate height has to be integrated over the column length L. Introducing the classical definition of H ($H=\sigma_x^2/L$), one then obtains for H [S7]:

$$H = \frac{\sigma_x^{\,2}}{L} = \int_0^1 H_{loc}(x') \cdot dx' \qquad \text{(S-23)}$$

wherein H represents the total (i.e., column length averaged) plate height. Under isocratic conditions, $H_{loc}(x')$ is a constant, so that Eq. (S-23) yields $H=H_{loc}$, as expected.

Knowing from Eqs. (S-16)-(S-17) that gradients runs with the same gradient steepness $\beta \cdot t_0$, t_{delay}/t_0 and ϕ_0 will subject the components to the same ϕ-value when reaching the same dimensionless position x' (x'=x/L) in the column, Eq. (S-23) now guarantees that gradient experiments conducted in columns with different length, but tested with the same component, can be expected to yield the same H, provided $\beta \cdot t_0$, t_{delay}/t_0 and ϕ_0 are the same. This holds for LSS as well as for non-LSS conditions (the validity of Eq. (S-19) was not needed in the above argumentation).

An additional effect occurring during gradient elution is the so-called “peak compression” [S6], caused by the fact that the rear of the solute plug experiences a higher concentration of organic modifier in the mobile phase than the front of the peak. This in turn causes the front of the band to experience a higher retention factor than its back and thus a higher retained species velocity for the back of the peak than the front, causing a reduction in solute band dispersion. Assuming the plate height in the column is constant during the gradient (and hence neglecting the effects discussed in Eqs. (S-20) to (S-23)), the average gradient plate height H_{grad} is related to the isocratic plate height H_{iso} by [S1,S5,S6]:

$$H_{grad} = H_{iso} \cdot G^2 \qquad \text{(S-24)}$$

where G is the so-called peak compression factor. It has been shown by Gritti and Guiochon [S5] for the case of both LSS and non-LSS systems that G only depends on the ϕ-history, as its value can be calculated as:

$$G^2 = \left(\frac{k_{elut}}{1 + k_{elut}} \right)^2 \cdot \frac{1}{\beta \cdot t_0} \cdot \int_{\phi_0}^{\phi_{elut}} \frac{[k(\phi) + 1]^2}{k(\phi)^3} \cdot d\phi \qquad \text{(S-25)}$$

It is only when the organic modifier is retained itself or when the local plate height strongly fluctuates during the gradient, that the dependency on the ϕ-history is less clear [S5].

For a component following the LSS-model, Eq. (S-25) reduces to [S6]

$$G^2 = \frac{1 + p + \frac{1}{3}p^2}{(1+p)^2} \qquad \text{with} \qquad p = \frac{k'(\phi_0)}{k'(\phi_0)+1} \cdot S \cdot \beta \cdot t_0 \qquad \text{(S-26)}$$

Under isocratic conditions, β=0, so that p=0 and G=1, and Eq. (S-24) reduces to $H_{grad}=H_{iso}$, as expected.

As can readily be seen from Eq. (S-25), G remains invariant as long as the component's gradient steepness $S\beta t_0$ is kept constant ($S \cdot \beta \cdot t_0$ is very often also denoted as 'b' or 'G' in literature [S2,S4,S7,S13-S15]). For example, when comparing a gradient run on one column and on two 2 coupled columns operated at the same mobile phase velocity, the time steepness β has to halve for the coupled system to have the same compression factor G (since $t_{0,2columns} = 2 \cdot t_{0,1column}$). This condition is in fact identical to that needed to keep the effect of the changing ϕ on the average plate height constant (cf. Eq. (S-23)). This of course greatly simplifies the conditions needed to keep a constant H when changing the column length.

In practice, the plate height under gradient conditions is influenced by even more factors, such as extra-column peak broadening (which can be measured and corrected for, although a distinction needs to be made for pre and post-column band broadening, see section 4.1 of the main article), viscous fingering effects (very steep gradients or step gradients), deviation of the retention behaviour from the LSS model (which also influences the value of G) and retention of the organic modifier [S5,S7]. One approach to account for these effects is to incorporate them into in Eqs. (S-24) and (S-23) as demonstrated in literature [S5]. This however requires complex calculations and a good knowledge of the relation between H varies and k', and, in turn, the relation between k' and ϕ. A common method used in literature to circumvent this problem is to lump all these factors into an empirical factor denoted as the J-factor (see Snyder et al.[S16,S17] for a set of approximate expressions for J and Neue et al. [S4] for a critical appraisal of this approach)[S4,S16,S17].

$$H_{grad} = H_{iso} \cdot (G \cdot J)^2 \qquad \text{(S-27)}$$

1.2) Illustration of the use of the plate height concept in gradient elution

Calculating the actual gradient plate height starting from the observed time-based peak width (or from N_{meas}) is in principle perfectly possible: provided one knows the k_{elut}-value corresponding to the observed k-value, Eq. (S-6) can be directly used to calculate the correct N. Generally, k_{elut} is not known, but this is not an impediment to carry out the method. In the present set of experiments for example, it was observed that the LSS-model was valid for the range of mobile phase composition experienced during the gradient and this then allowed to use Eq. (S-7) to calculate N, employing the experimental parameters given in Table S-1.

Table S-1: Linear solvent strength parameters experimentally determined for the different analytes by performing isocratic measurements of k' as a function of ϕ in the given range.

Component	$k'(\phi_0 = 0.5)$	S	ϕ range
Benzene	2.83	5.81	50-55
Naphthalene	7.16	6.88	50-65
Phenanthrene	17.22	7.48	50-75

In this way, the experimentally observed N_{meas}-data (or equivalently t_R^2/σ^2_t) were transformed into the plate height data (H=L/N) shown in Fig. S-1a. As can be noted, the thus obtained H versus u_0-curves nearly perfectly coincide, in agreement with the generally accepted assumption that the band broadening for components with an LSS elution behavior only depends weakly on the retention of the components [S6]. If the LSS-model would not have applied, a more intricate non-LSS model would have had to be used or k_{elut} could have been determined by performing an isocratic experiment with the mobile phase composition ϕ equal to ϕ_{elut}. The value of k_{elut} can then directly be determined as $k_{elut}=t_R/t_0-1$. Either of these methods anyhow requires additional experiments, but does not make the calculation of the gradient plate height fundamentally more difficult.

Fig. S-1b shows the obtained gradient plate heights H for benzene (shifted up by 3µm), naphthalene and phenanthrene (shifted down by 3µm) measured on different columns lengths. The represented plate height values are again obtained by starting from the N_{meas}-values calculated by the instrument software

and feeding them to Eq. (S-7) and (S-18) using the experimentally determined values of S. The +3 and -3 μm H-shifts in Fig. S-1 were made for clarity purposes, since otherwise the curves for the 3 components would overlap (similar to the curves shown in Fig. 1a).

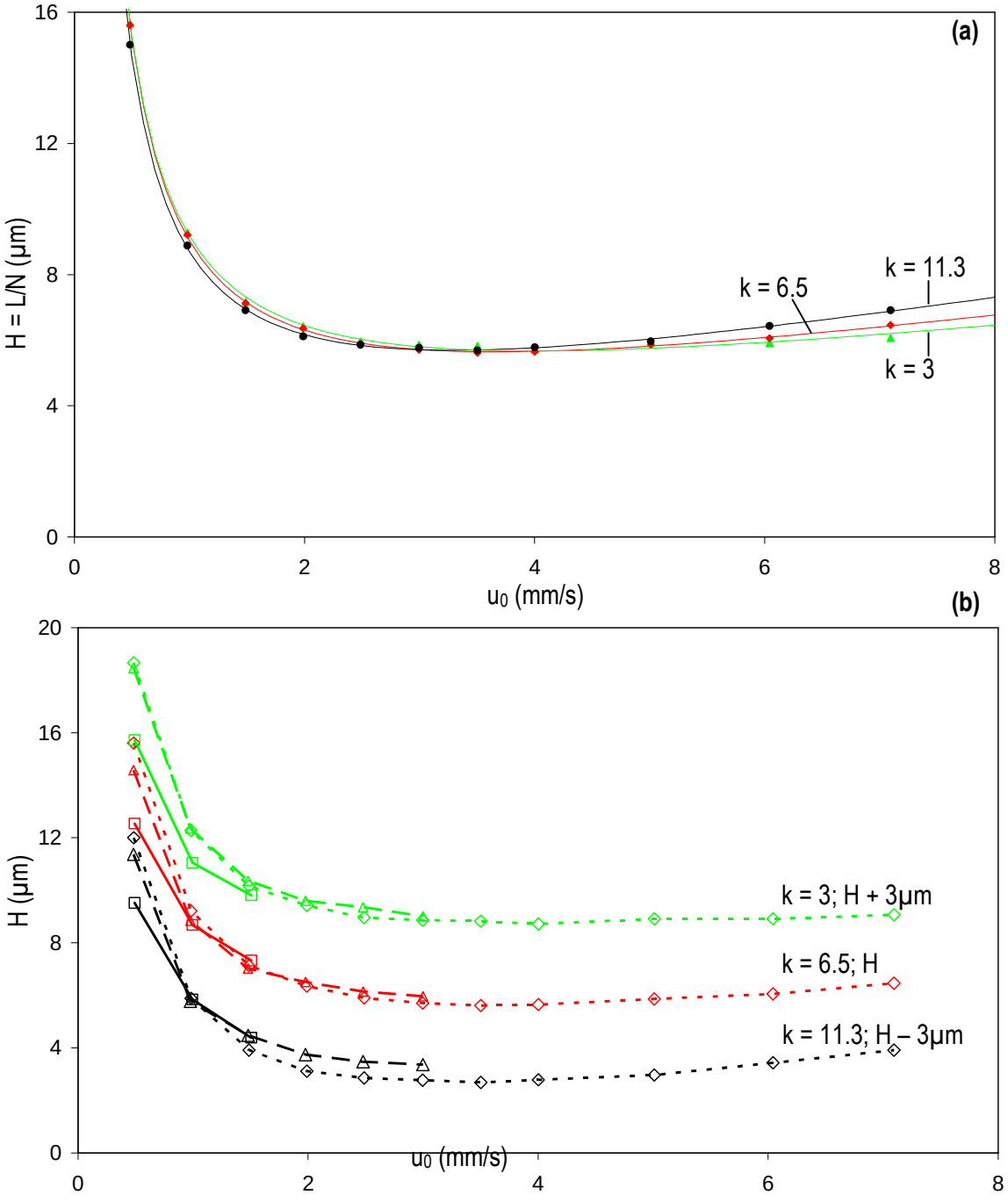

Figure S-1.(a) *Experimentally measured gradient plate height H, defined and calculated according to Eqs. (S-6) and (S-23), for a ACN/H_2O gradient elution with ϕ_0=0.5 and $\beta \cdot t_0$=0.016 for benzene (k=3, green data, ▲), naphthalene (k=6.5, red data, ♦) and phenanthrene (k=11.3, black data, ●) on a single (15cm) HALO column; Please note that different u_0-data points are obtained with a different β, so as to keep a constant $\beta \cdot t_0$.* ***(b)*** *Effect of the employed experimental column length on the measured gradient H, for three different column lengths (15 cm: ◊; 30cm: Δ; 60cm: □). For reasons of clarity, the curves for*

benzene (top, green curves) were shifted upward by 3µm, for phenanthrene (bottom, black curves) downward by 3µm. The naphthalene data (middle, red curve) were not shifted. Same gradient conditions as in Fig. 1a, keeping $\beta \cdot t_0$ fixed at 0.016 for the different columns lengths, as well as ensuring a constant t_{delay}/t_0.

The plate heights represented in Fig. S-1b have been calculated by adopting the length-independent H-conditions described in Section 1.1.2. Although the H-data points corresponding to the different column length systems overlap relatively well (which is needed to confirm H in its status of length-independent measure), Fig. S-1b also reveals some small differences. These differences can however be attributed to the fact that the 4 different columns used to construct the coupled column systems inevitably have a slightly different efficiency, and also have slightly varying t_0 and k values. The former results in a spread on the values for N_{meas}, whereas the latter affects the values of both k and k_{elut}. Especially these last two factors give rise to larger deviations since their contribution to N (or equivalently H) is squared (see Eq. (S-6)). In addition to the column to column variations, the corrections for the extra column contributions (and the error on this due to the focusing effect on the head of the column) and the inevitable errors on the experimental determination of the retention times, also introduces some errors that especially affect the most weakly retained compounds [S11].

Part 2: Necessary conditions underlying the validity of the kinetic performance limit-curve

The curves we commonly denote as kinetic plot curves [S18] in fact represent the kinetic performance limit of the support and mobile phase conditions under investigation. The present section investigates the conditions that need to be satisfied to turn a series of efficiency measurements conducted on a single column into the correct kinetic performance limit of the support filling that column.

Some of the expressions used further on are based on the concept of gradient plate heights. Although plate heights for gradient elution are not easy to calculate in practice, there is no fundamental impediment to use them. Furthermore, an approach is presented that circumvents the use of gradient plate heights (see Eqs. S-43 and following). It should also be noted that when we use the symbol H, this is consistently defined via eq. (S-18) and holds for isocratic as well as for gradient elution. In the latter case, H also incorporates the effect of peak compression.

2.1) Problem 1: Which condition should be satisfied to operate a given chromatographic system (with undetermined length) at its optimal kinetic performance limit, i.e., achieve a maximal N or n_p in a given time t_R, or, equivalently, achieve a given N or n_p in the shortest possible time t_R?

Theorem 1: *Each employed value of the mobile phase velocity u_0 leads to a point on the kinetic performance limit curve provided the u_0-value is obtained in a column operating under maximal pressure conditions ($\Delta P=\Delta P_{max}$). This holds for any value of u_0 and for gradient as well as isocratic conditions.*

Or, for any value of u_0: *case 1) $N = max(N)$ for a given $t_R \Leftrightarrow \Delta P = \Delta P_{max}$* (S-28a)

or: *case 2) $n_p = max(n_p)$ for a given $t_R \Leftrightarrow \Delta P = \Delta P_{max}$* (S-28b)

or: *case 3) $t_R = min(t_R)$ for a given N or $n_p \Leftrightarrow \Delta P = \Delta P_{max}$* (S-28c)

Proof:

- Case 1): combining Eqs. (7-9) from main article, it can be shown that:

$$N = \frac{\sqrt{\Delta P}}{H} \cdot \sqrt{\frac{t_0 \cdot K_v}{\eta}} \qquad \text{(S-29)}$$

In fact, Eq. (S-29) is simply a rewritten form of one of the two basic kinetic plot expressions (Eq. (6) of Desmet et al. [S18]). It shows that finding the maximal N under the constraint of a given t_0 corresponds to finding the conditions for which $\Delta P^{1/2}/H$ is maximal, or equivalently, for which $H/\Delta P^{1/2}$ is minimal. To find these conditions we need a way to express how H changes with t_0.

For this purpose, we first insert the result of Eq. (S-29) into Eq. (S-18) to calculate the column length and dividing the obtained expression by t_0 to obtain the velocity u_0:

$$u_0 = \frac{N \cdot H}{t_0} = \frac{\sqrt{\Delta P}}{H} \cdot \sqrt{\frac{t_0 \cdot K_v}{\eta}} \cdot \frac{H}{t_0} = \sqrt{\Delta P} \cdot \sqrt{\frac{K_v}{t_0 \cdot \eta}} \qquad \text{(S-30)}$$

Eq. (S-30) is again nothing but a rewritten form of one of the two basic kinetic plot expressions (Eq. (7) of Desmet et al. [S18]).

Noting now that the band broadening in most chromatographic systems can be represented by an expression of the form:

$$H = A(u_0) + \frac{B}{u_0} + C \cdot u_0, \qquad \text{(S-31)}$$

we can use the relation between u_0 and ΔP to write H as a function of the applied pressure. Noting that the only variable on the right hand side of Eq. (S-30) is ΔP (t_0 is a given constant in the presently considered case 1), these constants can be incorporated into the A-, B- and C-constants, so that we obtain a set of new constants A', B' and C':

$$H = A'(\sqrt{\Delta P}) + \frac{B'}{\sqrt{\Delta P}} + C' \cdot \sqrt{\Delta P} \qquad \text{(S-32)}$$

Dividing by $\Delta P^{1/2}$ then yields:

$$\frac{H}{\sqrt{\Delta P}} = \frac{A'(\sqrt{\Delta P})}{\sqrt{\Delta P}} + \frac{B'}{\Delta P} + C' \qquad \text{(S-33)}$$

Inspecting Eq. (S-33), or plotting it (see Fig. S-2), shows that $H/\Delta P^{1/2}$ decreases monotonically with $\Delta P^{1/2}$. This holds for any chromatographic system that is characterized by a plate height curve for which the A-term does not increase stronger than linearly with u_0 (or $\Delta P^{1/2}$) and ends in a C-term dominated regime where H does not increase stronger than linearly with u_0 (or $\Delta P^{1/2}$). For example, it can easily be verified that this holds for the three below models ($0<m<1$), covering nearly any possible chromatographic system [S11]:

$$H = A + \frac{B}{u_0} + C \cdot u_0$$

$$H = A \cdot u_0^{\,m} + \frac{B}{u_0} + C \cdot u_0 \qquad \text{(S-34)}$$

$$H = \left(\frac{1}{A} + \frac{1}{D \cdot u_0} \right)^{-1} + \frac{B}{u_0} + C \cdot u_0$$

Also the A-term expression proposed by Guiochon and Gritti [S19] leads to a trend as shown in Fig. S-2. It is only in some very special cases wherein the plate height curves display a convex upward trend in the high-velocity range that the $H/\Delta P^{1/2}$-curve does not decrease monotonically but goes through a minimum. Notable examples of this are the lack of a sufficiently high detector sampling rate or the occurrence of high-pressure viscous heating effects under non-adiabatic conditions [S20].

Now that we know from Eq. (S-29) that maximizing N corresponds to minimizing $H/\Delta P^{1/2}$, we can readily see from Fig. S-2 that the condition to obtain a maximal N at fixed t_0 corresponds to putting $\Delta P = \Delta P_{max}$.

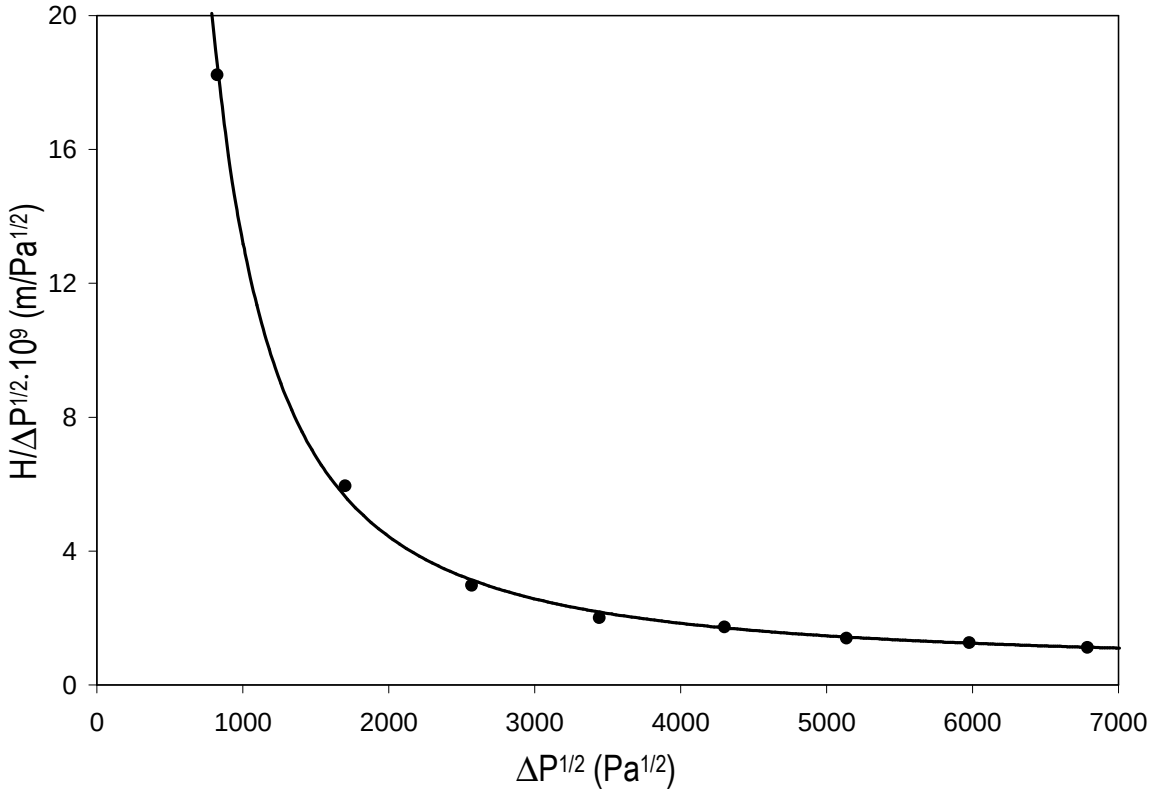

Figure S-2. *Plot of $H/\Delta P^{1/2}$ (•) versus $\Delta P^{1/2}$ for a fixed value of t_0 = 60s based on a set of H,u_0 data taken from the experimentally measured values of the isocratic elution of benzene on a single (15cm) HALO column (ϕ=0.504, k=2.76).*

Since we did not have to make any assumption on u_0 or the column length L, this condition holds for any value of $N<N_{max}$. N_{max} is the maximal number of plates that can be obtained with a given chromatographic system. N_{max} is obtained when u_0 tends to zero (i.e., N_{max} is obtained at the expense of an infinite separation time). This means that each value of u_0 can lead to a point on the kinetic performance limit, provided it is applied in a column with a length L selected such that $\Delta P=\Delta P_{max}$ (see also problem 2). This conclusion holds for isocratic as well as for gradient elution, as we did not have to make any assumption about the elution mode to arrive at it. To corroborate this further, it should also be noted that the integration on the right hand side of Eq. (S-32) does not change the general nature of its dependency on u_0 (or $\Delta P^{1/2}$).

- Case 2): Keeping all k_i- and $k_{elut,i}$-values the same, the expression for $n_{p,KPL}$ (see Eq. (S-52) further on) readily shows that maximizing n_p corresponds to maximizing the N_i-values appearing in each term of the summation the right hand side of Eq. (S-52). Since we know from case 1 that the necessary and sufficient condition to maximize N under the condition of a constant t_R or t_0 corresponds to operating the system at maximal pressure, it follows immediately that the same condition will also maximize each individual term of the summation, so that the total expression for n_p will also be maximal if $\Delta P=\Delta P_{max}$.

- Case 3): rewriting Eq. (S-29) into:

$$t_0 = \left(N \cdot \frac{H}{\sqrt{\Delta P}} \cdot \sqrt{\frac{\eta}{K_v}} \right)^2 \qquad \text{(S-35)}$$

it can readily be seen that minimizing t_0 (or t_R if k is kept the same) under the constraint of a given N again corresponds to minimizing $H/\Delta P^{1/2}$ (because η, N and K_v are assumed to be constant in Eq. (S-35)), which in turn corresponds to operating under $\Delta P=\Delta P_{max}$-conditions.

Since Eq. (S-52) shows that constraining n_p corresponds to constraining N, it again follows that the $\Delta P=\Delta P_{max}$-condition is necessary and sufficient to obtain a minimal t_0 or t_R for a given n_p.

2.2) Problem 2: How can the column performance that is measured at a given mobile phase velocity u_0 be translated into a point falling on the optimal kinetic performance limit?

***Theorem 2*:** *Irrespectively whether a column is operated under gradient or isocratic conditions, the column performance measured at any given mobile phase velocity u_0 can be transformed into a point on the kinetic performance limit (KPL)-curve provided the mobile phase viscosity (isocratic mode) or mobile phase viscosity history (gradient mode) and the corresponding plate height are independent of the column length and provided the given velocity u_0 is achieved in a column with maximal length L_{max}, i.e., by replacing ΔP by ΔP_{max} in Eq. (9) (see main article).*

$$\text{when } u_0 \text{ is fixed: } \Delta P=\Delta P_{max} \Leftrightarrow L=L_{max} \qquad \text{(S-36)}$$

Proof: Since the relation between H and u_0 is generally unknown, the only way to preserve the experimentally observed relation between the band broadening and the mobile phase velocity is to do the transformation at constant u_0 (so that the corresponding H also does not change). Let us now consider a given column performance data point measured at a given mobile phase velocity u_0, i.e., a data point that is measured by applying a pressure $\Delta P=\Delta P_{exp}$ in a column with length L_{exp}. When the mobile phase velocity u_0 and viscosity η are fixed, the only way to transform this data point into a point falling on the KPL-curve (requiring that $\Delta P=\Delta P_{max}$, see theorem 1) corresponds to maximizing L, i.e., by putting $L=L_{max}$ in Eq. (9) from the main article, because:

$$L_{exp}=\frac{K_v\cdot\Delta P_{exp}}{u_0\cdot\eta}\Leftrightarrow L_{max}=\frac{K_v\cdot\Delta P_{max}}{u_0\cdot\eta} \qquad \text{(S-37)}$$

The direct and linear relation between L and ΔP in Eq. (S-37) obviously holds only under the assumption that also η is independent of ΔP (see Problem 3 for a discussion of the conditions underlying this assumption).

The obtained experimental true column efficiency N_{exp} can also be transformed into a plate height H via:

$$N_{exp}=\frac{L_{exp}}{H} \qquad \text{(S-38a)}$$

Similarly, also the t_0-time is determined by the column length:

$$t_{0,exp}=\frac{L_{exp}}{u_0} \qquad \text{(S-38b)}$$

The key-factor to transform the data in Eqs. (S-38a-b) into their corresponding KPL-curve is the plate height H. Under isocratic conditions, H is a function of the following system variables:

$$H = H_{iso} = f(u_0, k, D_{mol}, \text{packing characteristics}) \qquad \text{(S-39a)}$$

Under gradient conditions, H is a function of the following system variables:

$$H = H_{grad} = f(u_0, k, D_{mol}, \text{packing characteristics}, S\beta t_0, G \text{ and } J) \qquad \text{(S-39b)}$$

In the latter case, some of the variables are also interdependent (e.g., D_{mol} and $S\beta t_0$)

Making now the obvious assumption that the KPL-curve is to be established for the same sample component(s) and mobile phase conditions as the one for which the experimental data set was obtained, and further assuming that H and η are independent of the column length and the applied pressure (see Problem 3), the only pressure-dependent variable in the whole set of kinetic performance determining expressions (Eqs. (7-9), see main article) is the column length. The only way to impose the $\Delta P=\Delta P_{max}$–condition needed according to Theorem 1 is then to maximize the column length:

$$\Delta P=\Delta P_{max} \Leftrightarrow L=L_{max} \qquad \text{(S-40)}$$

Denoting now the N-value that would be obtained when transforming the experimentally observed N into a N-value falling on the kinetic performance limit using the symbol N_{KPL}, and using the same subscript notation for t_0, it follows immediately that:

$$N_{KPL} = \frac{L_{max}}{H_{iso}} \text{ and } t_{0,KPL} = \frac{L_{max}}{u_0} \qquad \text{(S-41)}$$

Replacing now L_{max} by the right hand side of second equality in Eq. (S-37), we obtain an explicit expression for N_{KPL} and $t_{0,KPL}$ (explicit because they directly contain the H-value):

$$N_{KPL} = \frac{K_v \cdot \Delta P_{max}}{u_0 \cdot \eta \cdot H} \text{ and } t_{0,KPL} = \frac{K_v \cdot \Delta P_{max}}{\eta \cdot u_0^{\,2}} \qquad \text{(S-42)}$$

The reader will note that the expressions in Eq. (S-42) are identical to those obtained earlier for isocratic conditions [S18].

Introducing now the so-called column length rescaling factor, defined as:

$$\lambda = \frac{L_{max}}{L_{exp}}, \qquad \text{(S-43)}$$

and via Eq. (S-37) equal to:

$$\lambda = \frac{\Delta P_{max}}{\Delta P_{exp}}, \tag{S-44}$$

we can also turn the expressions in Eq. (S-31) into a set of implicit expressions (implicit because they do not directly contain the H-value):

$$N_{KPL} = \frac{L_{max}}{L_{exp}} \cdot \frac{L_{exp}}{H} = \lambda \cdot N_{exp} \text{ and } t_{0,KPL} = \frac{L_{max}}{L_{exp}} \cdot \frac{L_{exp}}{u_0} = \lambda \cdot t_{0,exp} \tag{S-45}$$

Knowing that $t_R=t_0(1+k)$, and assuming a constant k, a condition that anyhow needs to be made for H to be length-independent, Eq. (S-45) readily leads to the following explicit and implicit expressions for t_R:

$$t_{R,KPL} = \frac{K_v \cdot \Delta P_{max}}{\eta \cdot u_0^{\,2}}(1+k) \quad \text{and} \quad t_{R,KPL} = \lambda \cdot t_{R,exp} \tag{S-46}$$

The characterization of the separation efficiency under gradient elution conditions is usually done directly on the basis of the time-based peak widths (usually translated into the band standard deviation σ_t). Combining Eqs. (S-5) and (S-23), σ_t can however also be directly written as function of the gradient plate height as:

$$\sigma_t = \sqrt{L \cdot H} \cdot \frac{(1+k_{elut})}{u_0} \tag{S-47}$$

Starting from Eq. (S-47) and again replacing L by L_{max} in the same way as done in Eqs. (S-42) and (S-45), we obtain in the explicit form:

$$\sigma_{t,KPL} = \sqrt{\frac{\Delta P_{max} \cdot K_v}{u_0 \cdot \eta}} \cdot \sqrt{H} \cdot \frac{1+k_{elut}}{u_0} \tag{S-48}$$

In implicit terms, we obtain:

$$\sigma_{t,KPL} = \sqrt{L_{max} \cdot H} \cdot \frac{(1+k'_{elut})}{u_0} = \frac{\sqrt{L_{max}}}{\sqrt{L_{exp}}} \cdot \sqrt{L_{exp} \cdot H} \cdot \frac{(1+k_{elut})}{u_0} = \sqrt{\lambda} \cdot \sigma_{t,,exp} \tag{S-49}$$

Here, the beauty and the elegance of the implicit variant of the kinetic plot-expression becomes fully apparent, as one can directly calculate the band variance at the kinetic performance limit from the experimentally observed band variance.

Another frequently used performance characteristic is the peak capacity n_p. Starting from the piecewise-continuous definition given in Eq. (4) (see main article), Eq. (S-5) and the definition of k ($k=t_R/t_0-1$), it can be found that:

$$n_{p,exp} = 1+\frac{1}{4}\cdot\sum_{i=1}^{n}\sqrt{\frac{L_{exp}}{H_i}}\cdot\frac{k_i-k_{i-1}}{1+k_{elut,i}} = 1+\frac{1}{4}\cdot\sum_{i=1}^{n}\sqrt{N_i}\cdot\frac{k_i-k_{i-1}}{1+k_{elut,i}} = 1+\frac{1}{4}\cdot\sum_{i=1}^{n}\sqrt{N_{i,meas}}\cdot\frac{k_i-k_{i-1}}{1+k_i} \quad \text{(S-50)}$$

Wherein $n_{p,exp}$ is the experimentally observed peak capacity, and wherein H_i and $N_{meas,i}$ respectively are the plate height and the measured plate number for component i.

Performing the transformation from L_{exp} into L_{max} we can again obtain either an explicit or an implicit expression for peak capacity one can expect if the support and the operating conditions would be used at their KPL:

$$n_{p,KPL} = 1+\frac{1}{4}\cdot\sqrt{\frac{K_v\cdot\Delta P_{max}}{u_0\cdot\eta}}\cdot\sum_{i=1}^{n}\frac{1}{\sqrt{H_i}}\cdot\frac{k_i-k_{i-1}}{1+k_{elut,i}} \quad \text{(S-51)}$$

or:

$$\begin{aligned} n_{p,KPL} &= 1+\frac{1}{4}\cdot\frac{\sqrt{L_{max}}}{\sqrt{L_{exp}}}\cdot\sum_{i=1}^{n}\sqrt{\frac{L_{exp}}{H_i}}\cdot\frac{k_i-k_{i-1}}{1+k_{elut,i}} \\ &= 1+\frac{1}{4}\cdot\sqrt{\lambda}\cdot\sum_{i=1}^{n}\sqrt{\frac{L_{exp}}{H_i}}\cdot\frac{k_i-k_{i-1}}{1+k_{elut,i}} \\ &= 1+\frac{1}{4}\cdot\sqrt{\lambda}\cdot\sum_{i=1}^{n}\sqrt{N_i}\cdot\frac{k_i-k_{i-1}}{1+k_{elut,i}} \\ &= 1+\frac{1}{4}\cdot\sqrt{\lambda}\cdot\sum_{i=1}^{n}\sqrt{N_{i,meas}}\cdot\frac{k_i-k_{i-1}}{1+k_i} \end{aligned} \quad \text{(S-52)}$$

which upon inserting the expression for the experimentally observed peak capacity (i.e., that measured in a column with length L_{exp}) simply reduces to:

$$n_{p,KPL} = 1+\sqrt{\lambda}\cdot(n_{p,exp}-1) \quad \text{(S-53)}$$

Using the peak capacity based on the average peak variance ($\sigma_{t,av}=w_{p,av}/4$), a similar set of expressions can be derived:

$$n_{p,exp} = 1+\frac{t_{R,n,exp}-t_{0,exp}}{4\cdot\sigma_{t,av,exp}} \quad \text{(S-54)}$$

$$n_{p,KPL} = 1+\frac{(t_{R,n,exp}-t_{0,exp})\cdot\lambda}{4\cdot\sigma_{t,av,exp}\cdot\sqrt{\lambda}} = 1+\frac{(t_{R,n,exp}-t_{0,exp})\cdot\sqrt{\lambda}}{4\cdot\sigma_{t,av,exp}} = 1+\frac{(t_{R,n,KPL}-t_{0,KPL})}{4\cdot\sigma_{t,av,KPL}} \quad \text{(S-55)}$$

which upon inserting the expression for the experimentally observed peak capacity again reduces to:

$$n_{p,KPL} = 1 + \sqrt{\lambda} \cdot (n_{p,exp} - 1) \qquad \text{(S-56)}$$

an expression which is identical to Eq. (S-53).

Similarly, we can, starting from the expression for the resolution of a given critical pair:

$$R_s = \frac{t_{R,i} - t_{R,i-1}}{4 \cdot \frac{(\sigma_{t,i} + \sigma_{t,i-1})}{2}} \qquad \text{(S-57)}$$

write that:
$$R_{s,KPL} = \frac{\sqrt{L_{max}}}{2} \cdot \frac{k_i - k_{i-1}}{\sqrt{H_i} \cdot (1 + k_{elut,i}) + \sqrt{H_{i-1}} \cdot (1 + k_{elut,i-1})} = \sqrt{\lambda} \cdot R_{s,exp} \qquad \text{(S-58)}$$

or also:
$$R_{s,KPL} = \frac{1}{2} \cdot \frac{k_i - k_{i-1}}{\frac{(1 + k_{elut,i})}{\sqrt{N_i}} + \frac{(1 + k_{elut,i-1})}{\sqrt{N_{i-1}}}} = \frac{1}{2} \cdot \frac{k_i - k_{i-1}}{\frac{(1 + k_i)}{\sqrt{N_{i,meas}}} + \frac{(1 + k_{i-1})}{\sqrt{N_{i-1,,meas}}}} \qquad \text{(S-59)}$$

Since none of the above $L=L_{max}$-transformations relied on the assumption that the elution mode was isocratic or not, it can be concluded that the established expressions are valid under isocratic as well as gradient elution conditions.

2.3) Problem 3: Is the optimal kinetic performance limit independent of the length of the column in which the experimental column performance data were obtained?

Theorem 3: *Measurements of N, n_p or σ_t versus u_0 or t_0 conducted on columns with a different length lead to the same kinetic performance limit curve provided the measurements are conducted with the same component and the same mobile phase (isocratic elution) or the same mobile phase history parameters ϕ_0 and gradient steepness $\beta \cdot t_0$ (gradient elution), and provided the pressure- and viscous heating dependence of H, k and η are properly corrected for and provided adiabatic systems are considered.*

Proof:

The argumentations in theorem 1) and 2) are based on the assumption that H, k and η are length-independent. These are assumptions that are commonly made in LC. If they hold, a KPL-curve that is based on the measurements made in a given column with a given length will correctly predict the

performance at maximal pressure in a column with another length. However, conditions exist wherein the assumption of a length-independent H, k and η is too crude. Below is an overview of the conditions wherein this is the case.

For the isocratic elution mode, inspection of the variables between the brackets on the right hand side of Eq. (S-39a) shows that a length-independent H requires that experiments conducted in different column lengths should be performed with the same components and mobile phase, because this automatically also leads to the same k and D_{mol}-conditions. In addition also the packing characteristics should be length-independent. This assumption can never be perfectly met (an overview of possible length-depending packing effects was recently given by Guiochon [S3]), but is in many cases an acceptable approximation. Another length-dependency arises when the measured column performance data contain a significant extra-column contribution. A correction to the KPL-calculation procedure for the latter case has been proposed by Heinisch et al. [S21], although this correction is only valid for isocratic separations. In gradient elution, the analytes elute from the column with a smaller retention factor than the one they enter the column with. As a consequence, the contribution of the pre-column band spreading is reduced (focusing effect on the front of the column) the relevant extra-column band broadening contribution can no longer measured by simply short-circuiting the inlet and outlet connection tubing. Instead, more elaborate correction methods are needed.

And last but not least, also viscous heating effects can lead to a length-dependency of H [S12,S20]. Under perfectly adiabatic conditions (and with a column wall with a zero axial heat transport), the transcolumn velocity profile can be assumed to remain perfectly straight under viscous heating conditions, so that no additional H-contribution is created. The viscous heating might however alter the local D_{mol} and k_{loc} values experienced by the components when passing through the column because of the axial T-gradient that develops. As can be noted from Eq. (S-20), this will lead to a change in H as compared to the case wherein this axial T-gradient is absent, i.e., in the low pressure case. Under perfectly adiabatic conditions, this T-gradient is only dependent on the column pressure gradient, via [S20,S22]:

$$\Delta T = \frac{\Delta P \cdot (1 - \alpha \cdot T)}{C_p} \qquad \text{(S-60)}$$

Eq. (S-60) implies that the H-values for the low u_0-data points (measured at a low ΔP) will be less affected by an axial T-gradient than the high u_0-data (measured at a high ΔP). Since the kinetic plot method requires that all u_0-data points are transformed into a data point at the maximal pressure, it is straightforward to understand that the extrapolation of a low u_0-data point will not contain the same T-effect one can expect if the same u_0 would be obtained in a column operated at the maximal pressure. Fortunately, the T-effect is countered by the increase in column pressure ΔP (ΔP and T have an opposite effect on k_{loc} and D_{mol} values). As a consequence, and, as shown both theoretically and experimentally [S12,S20], this effect remains small for values up to 1000 bar, and probably even up to 2000 bar.

Under isothermal conditions on the other hand, the effect of viscous heating leads to a specific additional plate height contribution [S23-S25]. This plate height contribution only depends on u_0 and not on ΔP, so that the kinetic plot extrapolation from a low pressure to a high pressure simply preserves the measured effect and hence properly account for it. In normal bore columns, this additional plate height contribution however only reaches its constant value after a very long entrance length [S26], so that the plate heights observed in short columns might also be length-dependent. In addition, the pressure-dependency of k and D_{mol} might also introduce an unknown change in H, so that measurements conducted at the same u_0 but at different pressure would anyhow lead to a different H. Moreover, since the effect of ΔP is in this case not countered by an increase in T, the effect of ΔP on H can be expected to be larger in isothermal than in adiabatic conditions. Fortunately, isothermal conditions are anyhow to be avoided when operating under viscous heating conditions [S24]. The failure of the KPM under isothermal conditions should therefore not be considered a too huge problem, as this is not a practically relevant operating condition anyhow. For cases intermediate between isothermal and adiabatic, an intermediate pressure extrapolation accuracy can be expected.

The above mentioned limitations on the length-independency of H remain the same in the gradient elution mode. The only difference (see part I, section a.2) with the isocratic conditions is that now not only the same mobile phase composition needs to be used at the start (same ϕ_0), but that also the same gradient steepness βt_0 needs to be applied, implying that β needs to be halved when L is doubled ($\beta=[\phi_{tend}-\phi_0]/[t_{end}-t_{start}]$). In addition, also t_{delay}/t_0 needs to be kept constant. Fortunately, this is also the necessary condition to obtain the same k (see Eq. (S-16-17)) and the same peak compression (see Eq.

(S-25)). It is also the condition leading to the same effective η, as the local η is uniquely determined by the local ϕ, so that we can again write an expression that is similar to Eq. (S-23):

$$\eta = \int_0^1 \eta_{loc}(x') \cdot dx' \tag{S-61}$$

with the relation between ϕ and x' still determined by Eq. (S-17), and hence also only depending on the value of ϕ_0, t_{delay}/t_0 and $\beta \cdot t_0$.

Similar to the case of a length-independent H, the condition of a constant relative ϕ-history is not sufficient to obtain a length-independent η if also pressure and viscous heating effects come into play, because the viscosity of a liquid is known to be strongly temperature- and pressure-dependent (much stronger than H in most cases). This can for example be witnessed from Fig. 4 of Mazzeo et al., who reported measurements of an observed column permeability to describe the effect of ΔP and T on η [S27]. Fortunately, this effect can be measured experimentally and exactly accounted for, at least in an adiabatic system. In this case, the viscosity measured at the maximal pressure in any given column length will always be influenced by the same T-gradient (cf. Eq. (S-60)). As a consequence, the KPL-curve should be established with the η-value (explicit expressions) or the λ-value (implicit expressions) measured when $\Delta P = \Delta P_{max}$ (i.e., at the highest applied flow rate). In this case, the λ-values for the other flow rates or velocities can be obtained as follows:

$$\lambda(F) = \lambda_{F\,max} \cdot \frac{F_{max}}{F} = \lambda_{u_0,max} \cdot \frac{u_{0,max}}{u_0} \tag{S-62}$$

The fact that the viscosity continuously changes during a gradient elution run and might go through a maximum does not affect the general validity of this correction, as long as the different column length systems that correspond to the data points falling on the KPL-curve are subjected to the same mobile phase history.

In a perfectly isothermal system, the viscosity will only change via its dependency on the pressure, so that one should again calculate the KPL based on the viscosity observed at the highest experimental pressure. Eq. (S-62) hence remains valid under isothermal conditions. The correction given by Eq. (S-62) only becomes inaccurate if the thermal conditions of the system are in between isothermal and adiabatic and change with the column length.

Whereas the above discussion has been made for gradient conditions, no assumptions have been made that would invalidate Eq. (S-62) under isocratic conditions. Eq. (S-62) is hence valid under both isocratic and gradient elution conditions.

A fully similar argumentation can be made for the column length-independency of k. Since k depends on both T and ΔP, it is again the experimental k-value measured at $\Delta P = \Delta P_{max}$ that will be representative for all column length systems falling on the KPL-curve, provided the system behaves either perfectly adiabatic or isothermal. Intermediate situations are again more complex [S12].

Another potential source that can lead to length-dependent plate heights under gradient elution is the dwell volume (=instrument volume from mobile phase pump till column entrance). This introduces a delay time t_{delay}. As noted in Section 1.1.3, the potential length-dependent effect of this delay time on H can be circumvented by adding an additional delay time in the gradient run program to keep the ratio of t_{delay}/t_0 constant if the length L changes. The only shortcoming of this correction method is that it is not possible to give the same ϕ-history for columns shorter than the original one (since the dwell volume can normally not be reduced). There is however a more elegant method to eliminate the effect of the dwell volume on the gradient separation, if the HPLC instrument permits this, and that is a delayed injection [S28]. In this operating method, the mobile gradient is run as normal but the injection is halted till the pump has pumped a mobile phase volume equal to the dwell volume. This method is also convenient if the compared columns have a different inner diameter. In the presently experimentally investigated case, the overall effect introduced by the dwell volume on the observed peak capacity was however small (i.e., only small deviations were observed when performing the gradient method with or without correction for the dwell volume).

2.4) Illustration of the transformations underlying the gradient KPM

Fig. S-3 relates to the phenantrene data already shown in Fig. S-1 (black data points) and shows the data transformation (see added full line arrows) according to the explicit kinetic plot expressions, going from an experimental plate height plot (Fig. S-3a) to the corresponding kinetic performance limit (KPL) of the system (Fig. S-3b). As can be noted, the thus obtained KPL-curve is identical to that obtained via the implicit method (see dashed arrows), as one would expect for a consistent set of data transformation expressions. The implicit transformation is not influenced by any possible k_{elut}-estimation error, because

k_{elut} is simply not needed to do the transformation. The explicit transformation (Fig. S-3) is however also not influenced by any possible k_{elut}-error, because the possible error involved by going from σ_t or N_{meas} to H (needed to establish Fig. S-3a) is fully compensated when returning to the σ_t- or n_p-coordinates in the KPL (Fig. S-3b), provided the same k_{elut} is used. Hence the agreement between the explicit and implicit KPM will always be valid, even with an inaccurate estimation of k_{elut}. The implicit expressions are however exceedingly simpler to use than their explicit counterparts.

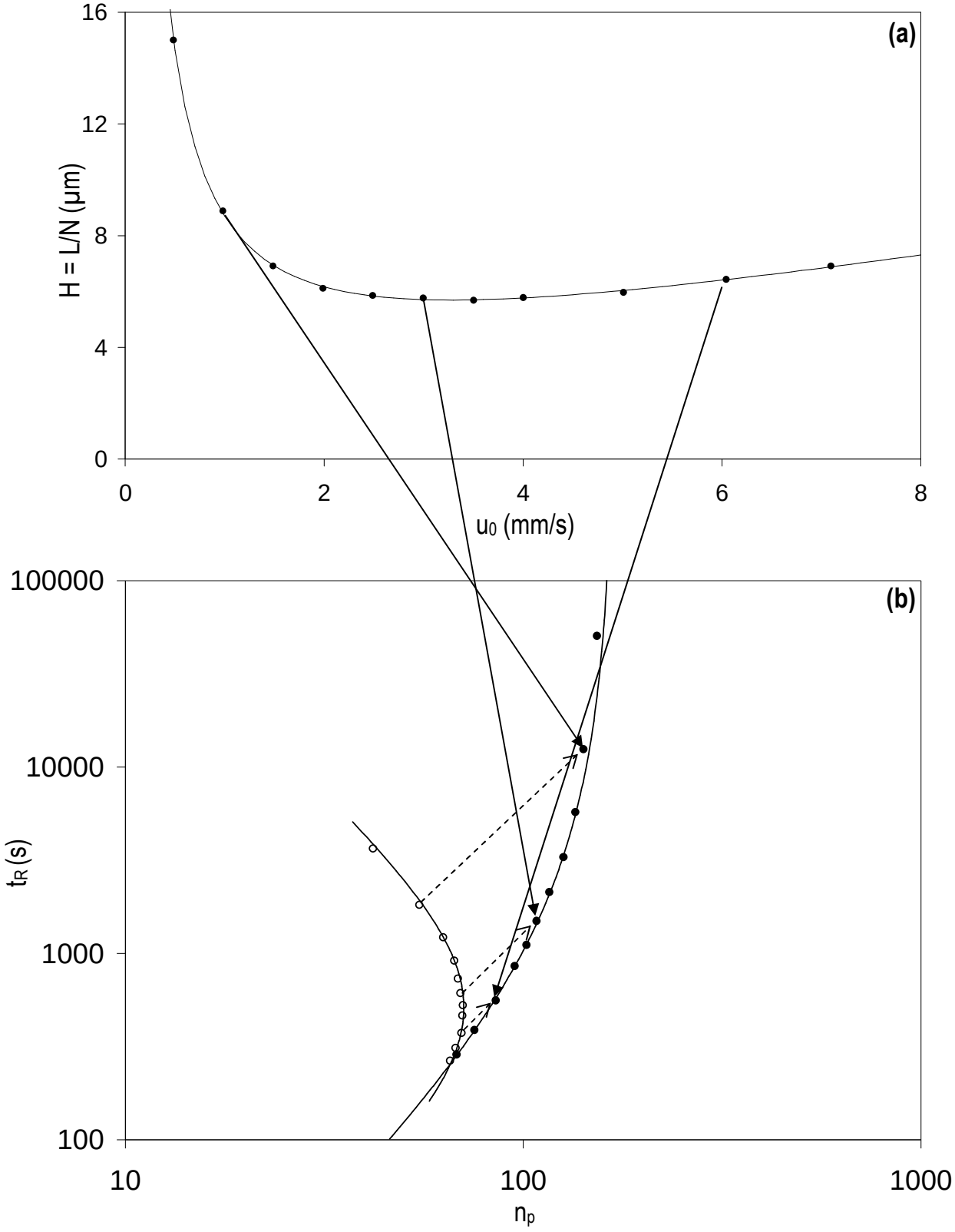
(a)
H = L/N (µm)
16
12
8
4
0
0
2
4
6
8
u0 (mm/s)
(b)
tR (s)
100000
10000
1000
100
10
100
1000
np

Figure S-3. *Data transformation (full arrows) according to the explicit kinetic plot expressions starting from* ***(a)*** *the experimental values of H versus u_0 for phenanthrene (same data as full black symbol data in Fig. S-1b) and transforming into* ***(b)*** *the corresponding kinetic performance limit (represented in terms of peak capacity n_p for phenantrene) of the system (ΔP_{max} = 600 bar). The open symbols and the dotted arrows in Fig. S-3b illustrate how the implicit expression result in the same KPL. Same experimental data as Fig. S-1.*

Figure S-4 illustrates how the point-by-point transformation of the experimental data to the KPL can be very easily implemented in a spreadsheet program such as Microsoft® Excel. Please note the list of KPL-variables shown in Fig. S-4 is not complete (see Eqs. (15-21) in the main MS for a more extensive list) and that more parameters are represented than strictly needed if one would want to establish only one type of KPL-curve.

	Experimental data									KPL					
F (ml/min)	t_0 (s)	t_R (s)	N_{meas}	N_{exp}	ΔP_{col} (bar)	σ_t (s)	n_p	λ	$t_{0,KPL}$ (s)	$t_{R,KPL}$ (s)	N_{KPL}	$\sigma_{t,KPL}$ (s)	$n_{p,KPL}$	L_{KPL} (cm)
				Eq. (S-6)			*Eq. (4)*	*Eq. (14)*	*Eq. (15)*	*Eq. (16)*	*Eq. (17)*	*Eq. (19)*	*Eq. (18)*	*Eq. (21)*
0.05	324.9	3655.8	32284	8597	43	20.35	46	13.95	4533.9	51010.6	119956	283.9	169	209
0.1	160.7	1821.6	55720	14838	88	7.72	60	6.85	1100.0	12472.0	101588	52.8	155	103
0.15	106.3	1219.3	73597	19598	128	4.49	69	4.71	500.3	5737.8	92227	21.2	148	71
0.2	79.7	915.1	83892	22339	167	3.16	73	3.59	286.1	3287.0	80246	11.3	138	54
0.25	63.8	733.0	87737	23363	206	2.47	75	2.91	185.8	2135.0	68049	7.2	127	44
0.3	53.1	612.7	90150	24006	246	2.04	76	2.44	129.4	1493.8	58527	5.0	118	37
0.35	45.5	527.4	92665	24676	285	1.73	77	2.11	95.9	1111.7	52016	3.7	111	32
0.4	39.8	464.0	92117	24530	325	1.53	77	1.84	73.5	855.9	45249	2.8	104	28
0.5	31.9	374.4	90973	24225	401	1.24	76	1.50	47.7	559.8	36217	1.9	93	22
0.6	26.5	311.0	84901	22608	481	1.07	74	1.25	33.1	388.4	28231	1.3	82	19
0.7	22.7	265.7	79614	21200	556	0.94	71	1.08	24.5	286.7	22877	1.0	74	16
$\Delta P_{col,max}$ (bar)		600			$k_{F = 0.7ml/min}$	11.59		$k_{elut,F=0.7ml/min}$	5.50		L_{exp} (cm)	15		

Figure S-4. *Example of a spread-sheet calculation procedure to transform a series of experimental kinetic performance data obtained on a column with given length into the corresponding KPL-values (data related to phenantrene, see Fig. S-3).*

Fig. S-5 shows 2 chromatograms corresponding to both ends of the full black arrow added to Fig. 1 of the main article. The chromatogram corresponding to the point on the fixed length KPL (open symbols on Fig. 1) is given in Fig. S-5a and was established on a single HALO column of 15cm. The chromatogram corresponding to the point on the KPL limit (for an experimental pressure of 527 bar) was determined using 4 coupled 15cm columns and is given in Fig. S-5b. As can be clearly observed, the retention times of the components increase with a factor of 4, as expected by the relation between the column lengths: $\lambda = L_{max}/L = 4$. The corresponding pressure drop also increases by the same factor of 4 as expected (except for some column to column variation in permeability) and the observed peak capacities (85 and 175 respectively) agree well with those expected from Eq. (18) or (S-53).

The overlaid gray chromatogram on Fig. S-5b (see peaks denoted with *) illustrates the effect of an inappropriate adjustment of the dwell time in gradient elution. By not inducing an additional delay time at the start of elution, the mobile phase gradient reaches the front of the column earlier and as a result, the elution window is decreased.

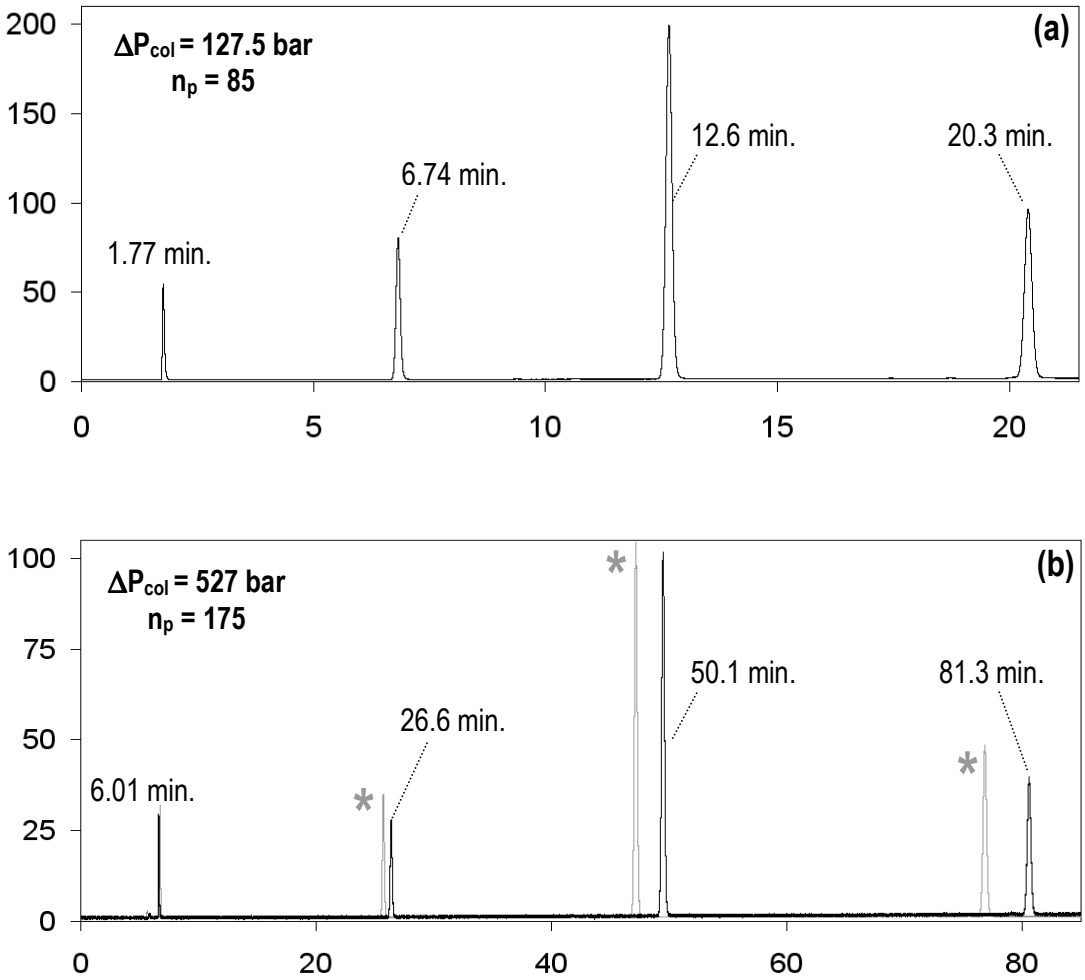

Figure S-5. *Chromatograms corresponding to the 2 ends of the full arrow on Fig. 1 in the main article (see caption Fig. 1 for experimental conditions, F = 0.15 ml/min):* ***(a)*** *single HALO column (15cm),* ***(b)*** *4 coupled HALO column (60cm) with appropriate adjustment of both $\beta \cdot t_0$ and t_{delay}/t_0 (black) and with the adjustment of $\beta \cdot t_0$ only, i.e. without correction on t_{delay} (gray, peaks denoted by an *).*

Symbols:

(only additional symbols for the SI are shown, see full list in main article)

A,B,C,D	coefficients in the plate height expressions [S29-S33], see Eq. (S-34)
A',B',C'	coefficients in the plate height expressions, see Eq. (S-32)
C_p	heat capacity of solvent, [J/(m³·K)]
D_{mol}	molecular diffusion coefficient, [m²/s]
G	peak compression factor, [/]
J	empirical factor, [/]
k_n	effective phase retention factor of last eluting component, [/]
m	coefficient in the general Knox equation, often taken as 1/3 (0 < m < 1), [/]
N_{meas}	measured or apparent plate number, see Eq. (S-3), [/]
T	temperature, [K]
t_{dwell}	system dwell time, [s]

Greek symbols:

α	thermal expansion coefficient of the mobile phase, [1/K]

Subscripts:

grad	gradient elution mode
iso	isocratic elution mode

References:

[S1] L.R. Snyder, D.L. Saunders, J. Chromatogr. Sci., 7 (1969) 195-208.

[S2] L.R. Snyder, J.W. Dolan, J.R. Gant, J. Chromatogr., 165 (1979) 3-30.

[S3] G. Guiochon, Chromatogr. A, 1126 (2006) 6–49.

[S4] U.D. Neue, D.H. Marchand, L.R. Snyder, J. Chromatogr. A, 1111 (2006) 32–39.

[S5] F. Gritti, G. Guiochon, J. Chromatogr. A, 1145 (2007) 67–82.

[S6] H. Poppe, J. Paanakker, M. Bronckhorst, J. Chromatogr., 204 (1981) 77–84.

[S7] U.D. Neue, J. Chromatogr. A, 1079 (2005) 153–161.

[S8] P.J. Schoenmakers, H.A.H. Billiet, R. Tussen, L. De Galan, J. Chromatogr. A, 149 (1978) 519-537.

[S9] F. Gritti, G. Guiochon, J. Chromatogr. A, 1212 (2008) 35–40.

[S10] F. Gritti, G. Guiochon, J. Chromatogr. A, 1178 (2008) 79–91.

[S11] U.D. Neue HPLC-Columns—Theory, Technology, and Practice; Wiley-VCH: Weinheim, 1997.

[S12] D. Cabooter, F. Lestremau, A. de Villiers, K. Broeckhoven, F. Lynen, P. Sandra, G. Desmet, J. Chromatogr. A, 1216 (2009) 3895-3903.

[S13] Y. Zhang, X. Wang, P. Mukherjee, P. Petersson, J. Chromatogr. A, 1216 (2009) 4597–4605.

[S14] X. Wang, D.R. Stoll, A.P. Schellinger, P.W. Carr, Anal. Chem., 78 (2006) 3406-3416.

[S15] U.D. Neue, J. Chromatogr. A 1184 (2008) 107–130.

[S16] J.D. Stuart, D.D. Lisi, L.R. Snyder, J. Chromatogr. 1989, 485, 657-612.

[S17] M.A. Stadalius, H.S Gold, L.R. Snyder, J. Chromatogr., 327 (1985) 2745.

[S18] G. Desmet, D. Clicq, P. Gzil, Anal. Chem., 77 (2005) 4058-4070.

[S19] F. Gritti, G. Guiochon, Anal. Chem. 78 (2006) 5329-5347.

[S20] U.D. Neue, M. Kele, J. Chromatogr. A, 1149 (2007) 236-244.

[S21] S. Heinisch,J.-L. Rocca, G. Desmet, J. Chromatogr. A, 1203 (2008) 124-136.

[S22] M. Martin, G. Guiochon, J. Chromatogr. A, 1090 (2005) 16–38.

[S23] G. Desmet, J. Chromatogr. A, 1116 (2006) 1116, 89–96.

[S24] A. de Villiers, H. Lauer, R. Szucs, S. Goodall, P. Sandra, J. Chromatogr. A, 1113 (2009) 84-91.

[S25] F. Gritti, G. Guiochon, J. Chromatogr. A, 1166 (2007) 47-60.

[S26] K. Broeckhoven, G. Desmet, J. Chromatogr. A, 1216 (2009) 1325–1337.

[S27] J.R. Mazzeo, U.D. Neue, M. Kele, R.S. Plumb, Anal. Chem., 77 (2005) 460A-467A.

[S28] U. D. Neue, Y.-F. Cheng, Z. Lu, "Fast Gradient Separations", in "HPLC Made to Measure: A Practical Handbook for Optimization", Stavros Kromidas, Ed., Wiley-VCH, Weinheim, 2006, pp. 47-58.

[S29] G. Desmet, K. Broeckhoven, Anal. Chem., 80 (2008) 8076–8088.

[S30] J.C. Giddings, Dynamics of Chromatography Part 1, Marcel Dekker: New York, 1965.

[S31] G. Guiochon, S. Golshan-Shirazi, A.M. Katti, Fundamentals of Preparative and Nonlinear Chromatography, Academic Press: Boston, 1994.

[S32] A. Berdichevsky, U.D. Neue, J. Chromatogr. 535 (1990) 189.

[S33] G. Desmet, K. Broeckhoven, J. De Smet, G.V. Baron, P. Gzil, J. Chromatogr. A, 1188 (2008) 71-188.